DETERMINATION OF SEISMIC ATTENUATION USING OBSERVED PHASE SHIFT IN SEDIMENTARY ROCKS

by
JEAN M. BARANOWSKI

B.S., University of Arizona
(1980)

SUBMITTED TO THE DEPARTMENT OF
EARTH AND PLANETARY SCIENCE
IN PARTIAL FULFILLMENT OF THE
REQUIREMENTS FOR THE DEGREE OF

MASTER OF SCIENCE IN GEOPHYSICS

at the
MASSACHUSETTS INSTITUTE OF TECHNOLOGY
May 1982

Signature of Author.....
Department of Earth and
Planetary Science

Certified by.....
M. Nafi Toksöz
Thesis Supervisor

Accepted by.....
Theodore R. Madden
Chairman, Department
Graduate Committee

DETERMINATION OF SEISMIC ATTENUATION USING OBSERVED PHASE SHIFT IN SEDIMENTARY ROCKS

by

JEAN M. BARANOWSKI

Submitted to the Department of Earth and Planetary Science on May 24, 1982 in partial fulfillment of the requirements for the Degree of Master of Science in Geophysics

ABSTRACT

Seismic attenuation has been measured in dry and water saturated samples of Berea sandstone, under varying pressure conditions. Ultrasonic P waveforms were studied to determine seismic quality factor, Q.

Two methods of data processing were used, both of which assume that Q is constant over the frequency range analyzed. The first is an amplitude spectral ratio technique, which involves comparing the amplitude spectrum of a rock sample waveform to the spectrum of an aluminum calibration standard.

Viscoelastic theory predicts that seismic attenuation must be accompanied by phase velocity dispersion. The second method of measurement exploits the model-dependent relationship between attenuation and dispersion to calculate Q from observed phase spectra. As with amplitudes, the phase spectrum of an aluminum standard is needed to cancel source and geometric effects.

Q is found to increase with pressure, and is lower for saturated than for dry samples. Q values determined from both methods are not systematically in agreement, particularly in cases where dispersion is slight over the narrow frequency range sampled.

Thesis Supervisor: Dr. M. Nafi Toksöz
Title: Professor of Geophysics

CONTENTS

I. INTRODUCTION

Amplitude spectral ratio methods are commonly used to measure seismic attenuation in laboratory experiments and seismic field studies (McDonal et al.,1958, and Toksöz et al., 1979). Mathematical modeling of seismic attenuation requires including velocity dispersion in order to satisfy causality. The same models postulate a specific relationship between velocity dispersion and attenuation.

More detailed discussions of the viscoelastic models that will be presented in this study are found in Toksöz and Johnston (1981), Bland (1960), Aki and Richards (1980) and Brennan and Smylie (1981).

The purpose of this study is to test a complimentary method of measuring attenuation using the phase velocity-attenuation relationship. Phase shift is measured as a function of frequency when the wave propagates a known distance. When phase shift can be measured accurately, this method may prove practical for measuring Q from seismic reflection data. The analysis also provides a test of the dispersion theory; if the material has significant attenuation, dispersion is more accurately measurable. In general, sedimentary rocks are more attenuating (lower Q) than igneous rocks and thus may provide a good medium for testing this theory.

Laboratory and field measurements of dispersion and its

relationship to attenuation in body waves has also been reported by Wuenschel(1965) and Ganley and Kanasewich(1980). They have found that measured dispersion is in agreement with viscoelastic models.

The form of phase velocity variation may also be used to investigate the mechanism of attenuation. Pore fluid influence on the elastic propetries of sedimentary rocks and semi-consolidated sediments are of primary interest in seismic exploration. Frequency dependence of Q in these materials may be modeled by the Biot effect (Biot,1956), taking into account the relative motion of the fluid and solid components. The Biot effect is predicted to become dominant at lower frequencies for media with low Q.

The data for this study consists of P waveforms recorded with ultrasonic laboratory apparatus, using Berea sandstone under varying pressure and saturation conditions. Vertical seismic profiling data would also be compatible with a very similar analysis.

Attenuation calculated using amplitude spectral ratios can be compared with that calculated using phase velocity, as a check on the theory and the internal consistency of data analysis.

II. DEFINITIONS

Standard definitions of Q (seismic quality factor) are usually given as (2.1) energy loss per deformation cycle,

$$\frac{1}{Q} = \frac{-\Delta E}{2\pi E} \tag{2.1}$$

where E is the total energy in a cycle or (2.2) in terms of the phase lag between stress and strain,

$$\frac{1}{Q} = \tan \delta \tag{2.2}$$

where $\tan \delta = \mathrm{Im}(M(\omega))/\mathrm{Re}(M(\omega))$, $\tan \delta$ is the internal friction coefficient and $M(\omega)$ is a complex modulus function relating stress and strain.

To show the equivalence of these definitions, and to cast them in a form useful for data analysis, one first expresses equation (2.1) in terms of wave amplitude rather than energy. Since for linear media,

$$E \alpha A^2$$

then:

$$\Delta E \alpha 2A\Delta A$$

and

$$\frac{1}{Q} = \frac{\Delta A}{\pi A} . \tag{2.3}$$

Now ΔA is the amplitude difference from one cycle to the next; it can be expressed in differential form as

$$\Delta A = \lambda \frac{dA}{dx} \tag{2.4}$$

where λ is the wavelength. Substituting for wavelength in terms of phase velocity, c, yields $\lambda = 2\pi c/\omega$. Hence,

$$\frac{1}{Q} = \frac{-dA}{dx}\frac{2c}{A\omega} \tag{2.5}$$

$$\frac{dA}{A} = \frac{-\omega}{2Qc}\,dx \quad . \tag{2.6}$$

One dimensional wave propagation in the x-direction has been assumed. Integrating equation (2.6) and solving for A,

$$\begin{aligned} A(x) &= A_0 \exp\{-\omega x/2Qc\} \\ &= A_0 \exp\{-\alpha x\} \ , \end{aligned} \tag{2.7}$$

which defines the attenuation coefficient, $\alpha = \omega/2Qc$.

The complex modulus $M(\omega)$ can be related to Q by reference to the complex wavenumber K, where

$$K(\omega) = \frac{\omega}{c(\omega)} + i\,\alpha(\omega) \ . \tag{2.8}$$

From the one-dimensional wave equation,

$$\rho\ddot{u} = \frac{\partial \sigma}{\partial x} \ , \tag{2.9}$$

where ρ = density, u = displacement in the x-direction, and σ = stress, substituting:

$$\sigma(\omega) = M(\omega)\cdot\varepsilon(\omega) = M(\omega)\,\partial u/\partial x. \tag{2.10}$$

Assume a solution of the form $u \alpha \exp\{i(Kx-\omega t)\}$:

$$\rho\omega^2 = K^2 M(\omega) \quad . \tag{2.11}$$

Then

$$M(\omega) = \frac{\rho\omega^2}{K^2} = \frac{\rho\omega^2}{(\omega/c(\omega) + i\alpha(\omega))}$$

$$= \frac{c^2(\omega)\rho}{(1 + i/2Q)} \quad . \tag{2.12}$$

Taking the ratio of real and imaginary parts,

$$\frac{Im(M)}{Re(M)} = -Q/(Q^2-.25) \sim -1/Q \quad . \tag{2.13}$$

Note that the approximation requires $Q >> 1/2$. For Q on the order of 10, for example, a .25% error is introduced, but Q is not considered measurable to such an accuracy in geologic materials.

III. ATTENUATION-DISPERSION THEORY

Attenuation (Q) of seismic waves has been reported by many investigators to be constant over a large frequency range; i.e., $\alpha(\omega)$ is approximately linear with frequency. Examples available in the geophysical literature are numerous; see, for example, Knopoff(1964), Gardner et al.,(1964), Gordon and Davis(1968), and Toksöz et al.(1979).

Mathematical models of attenuation that fit this common observation require velocity dispersion in order to produce physically possible pulse propagation; i.e., to satisfy causality.

As shown by Stacey(1975), if a delta function is the input, and it travels a time T in a medium with both Q and c (phase velocity) constant, the attenuated spectrum is:

$$F_t(\omega) = \exp\{-\omega T/2Q - i\omega T\} \qquad (3.1)$$

or, in the time domain,

$$f_t(t) = \frac{1}{2\pi}\int_{-\infty}^{\infty} F_t(\omega)\exp\{i\omega t\}d\omega$$

$$= \frac{1}{\pi}\cdot\frac{T/2Q}{(T/2Q)^2 + (T-t)^2} \cdot \qquad (3.2)$$

In this equation it can be readily seen that $f_t(0)\neq 0$; that is, the derivation implies non-causality. This attenuated pulse peaks at t=T and is symmetric about T; half the energy

has arrived before the assumed velocity predicts. Observation predicts sharp rise times and longer fall times. Clearly the assumptions have violated physical reality somewhere. Models allowing velocity dispersion have been formulated that do not encounter this contradiction.

Models that have been proposed are based on causality criteria. In general, assuming a wave number of the form given in equation (2.8),

$$K(\omega) = \frac{\omega}{c(\omega)} + i\alpha(\omega)$$

and requiring causality,

$$u(x,t) = 0 \qquad \text{for} \quad t < x/c(\infty)$$

implies that any attenuation-dispersion pair relationship must satisfy:

$$\frac{\omega}{c(\omega)} = \frac{\omega}{c(\infty)} + H[\alpha(\omega)] \tag{3.3}$$

(Aki and Richards, 1981) where $H[f(\omega)]$ is the Hilbert transform, defined by:

$$H[f(\omega)] = \frac{1}{\pi} \int_{-\infty}^{\infty} \frac{f(\omega')}{(\omega' - \omega)} \, d\omega' \, . \tag{3.4}$$

The Hilbert transform returns the function with a $\pi/2$ phase advance to all components. A causality relation analagous to

equation (3.3) in circuit theory is known as the Kramers-Kronig dispersion relation.

From equation (3.3), therefore, and the definition of Q (equation (2.7)), this requires

$$\frac{\omega}{c(\omega)} = 2Q\alpha(\omega) = \frac{\omega}{c(\infty)} + H[\alpha(\omega)] \qquad (3.5)$$

One function set which satisfies (3.5) that was suggested by Azimi et al.(1968), assumes that $\alpha(\omega)$ is almost linear with frequency, except at very high frequencies:

$$\alpha(\omega) = \frac{\alpha_0 \omega}{1 + \alpha_1 \omega} \qquad (\alpha_1 \omega << 1) \qquad (3.6a)$$

$$H[\alpha(\omega)] = \frac{2\alpha_0 \omega}{\pi(1-\alpha_1^2\omega^2)} \ln[1/\alpha_1\omega] \; . \qquad (3.6b)$$

The corresponding dispersion has been found to agree with many seismic observations (Brennan and Smylie,1981), and this form of $\alpha(\omega)$ has become widely accepted in recent seismological literature.

The phase velocity is found from (3.5) and (3.6):

$$\frac{\omega}{c(\omega)} = \frac{\omega}{c(\infty)} + \frac{2\alpha_0 \omega}{\pi(1-\alpha_1^2\omega^2)} \ln[1/\alpha_1\omega] \qquad (3.7)$$

or, neglecting $(\alpha_1\omega)^2$,

$$\frac{1}{c(\omega)} = \frac{1}{c(\infty)} + \frac{2\alpha_0}{\pi} \ln[1/\alpha_1\omega] \; . \qquad (3.8)$$

Taking a ratio of phase velocities at two different frequencies,

$$\frac{c(\omega_2)}{c(\omega_1)} \simeq 1 + \frac{2\alpha_0 c(\infty)}{\pi} \ln[\omega_2/\omega_1]$$

$$\simeq 1 + \frac{1}{\pi Q} \ln[\omega_2/\omega_1] \qquad (3.9)$$

where terms of order greater than 1/Q are neglected.

A recent thorough discussion and comparison of many attenuation models can be found in Brennan and Smylie(1981). As they have pointed out, although many models have been derived from various mechanisms, most give basically equivalent attenuation-dispersion relations. Models can be considered either a)empirical; worked out to satisfy causality and the known attenuation response of the medium, or b) based on an assumed form of the medium's viscoelastic behavior.

An approach to attenuation modeling based on viscoelasticity uses frequency dependent stress-strain functions formulated in terms of creep-relaxation mechanisms. The creep function is defined as the strain response to application of a constant stress. Conversely, the relaxation function is the stress response to a unit step of strain. That is, if

$$\sigma(t) = u(t)$$

$$\text{then} \qquad \varepsilon(t) = \psi(t), \qquad (3.10)$$

where: $u(t) = \begin{cases} 0, & t<0 \\ 1, & t\geq 0 \end{cases}$

$\psi(t)$ = creep function

$\sigma(t)$ = stress

$\varepsilon(t)$ = strain.

Similarly, if

$$\varepsilon(t) = u(t)$$

then $$\sigma(t) = \Phi(t), \tag{3.11}$$

where: $\Phi(t)$ = relaxation function.

To relate the creep-relaxation functions to the complex modulus, consider a time domain version of equation (2.10);

$$\sigma(t) = m(t)*\varepsilon(t). \tag{3.12}$$

Substituting from equation (3.11),

$$\Phi(t) = m(t)*u(t) = \int_0^\infty m(t-\tau)d\tau \tag{3.13}$$

or, $$\frac{d\Phi(t)}{dt} = m(t). \tag{3.14}$$

Then $$M(\omega) = \{F(\dot{\psi}(t)\}^{-1} \tag{3.15}$$

where F denotes the Fourier transform.

The inverse relationship to equation (3.12) defines the complex compliance function, s(t):

$$\varepsilon(t) = s(t)*\sigma(t), \tag{3.16}$$

so that there is a corresponding relationship with creep:

$$\frac{d\psi(t)}{dt} = s(t). \qquad (3.17)$$

Once a form for the function $M(\omega)$ is found, then, analagous versions of the classical one-dimensional wave equation are found by substituting the frequency dependent elastic modulus in equation (2.10).

Here two proposed creep functions and their corresponding dispersion relations will be discussed. The Lomnitz(1956) logarithmic creep law is based on laboratory data. In the notation used above, the creep function becomes:

$$\psi_L(t) = \frac{\sigma_0}{M}\left(1 + q\ \ln(1+at)\right),\ t \geq 0 \qquad (3.18)$$

where: M = elastic modulus

σ_0 = initial stress

a = high frequency limit

q = constant determined in laboratory measurements.

Aki and Richards(1980) have shown that this type of creep function results in an approximate dispersion relation equivalent to the Azimi(1968) relation noted earlier(3.9):

$$\frac{c(\omega_1)}{c(\omega_2)} = 1 + \frac{1}{\pi Q}\ln(\omega_1/\omega_2)$$

where $Q \simeq 2/\pi q$, $Q>>1$, and ω_1, ω_2 are different seismic frequencies.

Another creep law has been proposed by Kjartansson (1981), formulated to result in frequency-independent Q. This function is basically a power law:

$$\psi_k(t) = \frac{1}{M_0 \Gamma(1+2\gamma)} \left|\frac{t}{t_0}\right|^{2\gamma} \quad , t>0. \tag{3.19}$$

Then: $$M(\omega) = M_0 (\omega/\omega_0) e^{i\pi\gamma} \quad , \omega>0. \tag{3.20}$$

where ω_0, t_0 are any reference frequency and time, and γ is the exponent to be fit to the power law. Note that the argument of the modulus is independent of ω. From equation (2.2) therefore,

$$\frac{1}{Q} = \tan(\pi\gamma). \tag{3.21}$$

The dispersion formula is found by substitution into equations (2.8) and (2.11):

$$\frac{\omega}{c(\omega)} + i\alpha(\omega) = \frac{\omega}{c(\omega)}(1 + i/2Q)$$

$$= \omega(\rho/M_0)^{1/2} (\omega/\omega_0)^{-\gamma} e^{i\pi\gamma/2} \tag{3.22}$$

Therefore, $$c(\omega) = (M_0/\rho)^{1/2} (\cos(\pi\gamma/2))^{-1} (\omega/\omega_0)^{\gamma}$$

$$= c_0(\omega/\omega_0)^{\gamma} = \text{phase velocity} \tag{3.23}$$

and $$\alpha(\omega) = (\omega/c(\omega)) \tan(\pi\gamma/2) \qquad (3.24)$$

$$= \text{absorption coefficient.}$$

One fundamental difference between these two formulations is that the Kjartansson relation assumes no instantaneous elastic response; for high Q the response becomes "almost" instantaneous. Approximations show the relationship between the two dispersion laws. Expanding (3.23) in a Maclaurin series,

$$c(\omega) \alpha (\omega/\omega_0)^{\gamma} \simeq 1 + \gamma \ln(\omega/\omega_0) + \ldots$$

where terms of order $(\gamma \ln(\omega/\omega_0))^2$ and higher have been neglected. Since $\gamma \sim 1/\pi Q$ for high Q and the frequency range of a given observation will generally not be large, the Azimi and the Kjartansson dispersion laws can be seen as equivalent for high Q. Similarly, expansion of Futterman's (1962) dispersion law gives the same expression for phase velocity as equation (3.9).

Sedimentary rocks can be highly attenuating (low Q). Therefore in the work described here the dispersion relation of equation (3.23) is used.

IV. APPLICATION TO LABORATORY DATA

The initial data set consists of P waveforms recorded after propagation through laboratory rock samples or an aluminum calibration sample. Assuming that the waveform generation, propagation, and recording system can be modeled as a linear system, output waveforms can be expressed by:

$$O_a(t) = S(t)*P_a(t)*U(t-(t_a+t_0)) \quad (4.1)$$

$$O_r(t) = S(t)*P_r(t)*U(t-(t_r+t_0)) \quad (4.2)$$

where:

$O(t)$ = output waveform (a-aluminum, r-rock)

$*$ = convolution operator

$P(t)$ = effects introduced by propagation through the medium

$S(t)$ = effects introduced by the system: includes source waveform, transducer coupling, recording instrument effects. These are assumed to be the same for the aluminum standard and rock samples.

$U(t-t_i) = 0, \; t < t_i$

$\quad\quad\quad 1, \; t > ti$

t_a = travel time through the aluminum calibration sample

t_r = travel time through the rock being tested

t_0 = travel time through the system components, not

including the sample (or standard) itself.

In the frequency domain, then,

$$O_a(\omega) = S(\omega)\, P_a(\omega)\, e^{-i\omega(t_a+t_0)} \tag{4.3}$$

$$O_r(\omega) = S(\omega)\, P_r(\omega)\, e^{-i\omega(t_r+t_0)} \tag{4.4}$$

To get the desired expression for the propagation effects introduced by the rock medium, rearrange equations (4.3) and (4.4),

$$P_r(\omega) = P_a(\omega)\, \frac{O_r(\omega)}{O_a(\omega)}\, e^{-i\omega(t_r-t_a)} \quad . \tag{4.5}$$

Since aluminum has been observed to have Q values on the order of 150,000 (Zamanek and Rudnick, 1961) , it will be assumed to be nondispersive and nonabsorptive compared to the rock. This is equivalent to assuming that propagation through the aluminum does not change any of the source amplitude or phase information, i.e.,

$$P_a(f) = 1 \quad . \tag{4.6}$$

Rewriting equation (4.5) using amplitude and phase representations,

$$|a_{pr}(\omega)|\, e^{i\phi_{pr}(\omega)} = e^{-i\omega(t_r-t_a)}\, \left|\frac{a_{or}(\omega)}{a_{oa}(\omega)}\right|\, \frac{e^{i\phi_{or}(\omega)}}{e^{i\phi_{oa}(\omega)}} \tag{4.7}$$

where p subscripts refer to propagation effects and o

subscripts to observed outputs.

It is by equating the amplitudes in (4.7) that Q values are calculated with amplitude spectra,

$$|a_{pr}(\omega)| = |a_{or}(\omega)|/|a_{oa}(\omega)| \quad . \tag{4.8}$$

Each amplitude can be described by a function of the form,

$$a(\omega) = A_m(x)\exp\{-\alpha_m(\omega)x\} \tag{4.9}$$

where x is the propagation distance and A_m depends on the geometry of the medium being tested. Since the sample and standard are of the same dimensions and are tested using the same laboratory equipment, it will be assumed that the function A_m is not frequency dependent. Then α_m is found by taking the ratio of Fourier amplitudes:

$$\frac{|a_{or}(\omega)|}{|a_{oa}(\omega)|} = \frac{A_r}{A_a}\, e^{-(\alpha_r-\alpha_a)x} \tag{4.10}$$

or,

$$\ln\left|\frac{a_{or}(\omega)}{a_{oa}(\omega)}\right| = \ln\left|\frac{A_r}{A_a}\right| - (\alpha_r-\alpha_a)x \tag{4.11}$$

(Toksöz et al.,1979). Since $\alpha=\omega/2Qc$ and $Q_a>>Q_r$, α_a can be neglected and Q_r can be found from the slope of a line fitted to $\ln|a_{or}(\omega)/a_{oa}(\omega)|$ vs. frequency.

By equating the phases in (4.7)

$$\phi_{pr}(\omega) = \phi_{or}(\omega) - \phi_{oa}(\omega) - \omega(t_r - t_a) \pm 2\pi n \qquad (4.12)$$

where n is an integer. Phase velocity is defined by $c(\omega)=\omega/k$, where k is the wavenumber, which is constant in this case. ω is related to the inverse of the time delay for each frequency component, $\omega = 2\pi/t$, where t is the delay for the individual frequency. Then, $\phi_{pr}(\omega)/\omega + t_r$ = delay, for a given frequency. The phase velocity can then be calculated from the measurable quantities in equation (4.12) by:

$$C(\omega) = \frac{x\omega}{\phi_{pr}(\omega)+\omega t_r}$$

$$= \frac{\omega x}{\phi_{or}(\omega) - \phi_{oa}(\omega) + \omega t_a \pm 2\pi n} \quad . \qquad (4.13)$$

From equation (4.13) phase velocities are calculated using the observed ouput phase spectra from rock samples and an aluminum standard of the same length. Since the phase could equivalently be equal to the determined value plus or minus a multiple of 2π there is a degree of nonuniqueness in the phase spectrum. In practice, this has not been a problem since the group velocity is quite well known and only a single value of n gives reasonable phase velocities. Phase

unwrapping is done using the algorithm developed by Tribolet (1977).

Equations (4.11) and (4.13) then, are the basis for the computational procedure. The P and S waveforms are digitized as 1024 point time series with a sampling rate of 100 nanoseconds.

The Fortran software used in this analysis was written by Mark Willis (Willis, 1982) for borehole seismology applications; it required only minor modifications to be applied to ultrasonic data.

The waveforms are first windowed to include only the first few cycles, thereby removing later arrivals which are due to reflections within the medium and the system. A 15 point sine taper is applied to the edges of the windowed waveform.

To measure attenuation from amplitude spectra, two time series, corresponding to the standard and sample waveforms, are Fast Fourier Transformed. The two amplitude spectra are plotted along with a plot of the log of their spectral ratios vs. frequency. The user interactively defines a frequency window, and Q is found from the slope of the best fit least squares line fit over the window. From equation (4.11) the slope is equal to α_r; since the velocity has been measured Q is found from $\alpha=\omega/2cQ$. The determined Q turns out to be somewhat sensitive to the window chosen, so

the results were standardized by using window cutoffs defined by 25% of the maximum amplitude in the rock.

For phase velocity determination, the phase spectra of the same pair of windowed waveforms is used to calculate phase velocity, using equation (4.13) and the measured travel time in the aluminum calibration. Phase velocities are plotted simultaneously for three different values of the integer constant n. The criteria used for choosing a value of n were: minimum dispersion and velocity near the velocity measured in the lab.

The appropriate dispersion curve is then used to calculate Q vs. frequency based on the dispersion relation, equation (3.23):

$$c/c_0 = (\omega/\omega_0)^{\frac{1}{\pi}(\tan^{-1}(1/Q))} \qquad (4.14)$$

Taking logarithms of both sides and solving for Q,

$$Q = \cot\left[\pi\left(\ln(c(\omega))-\ln(c_0)/\ln(\omega)-\ln(\omega_0)\right)\right] \qquad (4.15)$$

$Q(\omega)$ calculated from equation (4.15) is plotted with the dispersion curve and the rock amplitude spectrum, removing the singularity at ω_0 by averaging around it. The choice of ω_0 is a source of ambiguity; theoretically it is any reference frequency for which the phase velocity is known. The energy bandwidth of the amplitude spectrum is fairly narrow, and any

c_0, ω_0 pair must come from the data within this range. It might be preferable to have a reference velocity corresponding to a known frequency outside the bandwidth. It would therefore be useful to perform the same experiments with varying transducer resonant frequencies. However, the data acquisition apparatus currently precludes this.

The calculation of equation (4.15) can get unstable when dispersion is small. The reference frequency used in the reported results was 1 MHz. This is the resonant frequency of the transducers and is above the frequency corresponding to the maximum of the experimental amplitude spectra. Since the least variation in phase velocity occurs at high frequency, it seems reasonable to assume an ω_0 in this range. Although the choice of ω_0 is presumably arbitrary, the same ω_0 was used consistently for all results.

V. RESULTS

The analysis described in the previous section has been performed on waveforms recorded by Karl Coyner (Coyner, 1982) at MIT. The rock was Berea sandstone, tested under both oven dry and distilled water saturated conditions. Data recorded with differential pressures of 100, 250, and 450 bars were analyzed.

The resulting Q values calculated for P waves are summarized in Table 1 and Figure 1. For dry samples, Q calculated from amplitude spectral ratios (Q_{pa}) increases monotonically with increasing pressure. Q calculated from dispersion (Q_{pd}) increases for the lower pressures but is apparently low for the higher pressure. This discrepancy may be related to a difference in filter settings on the recording electronics.

For the other five comparisons the high pass filter in the recording system was set with the same band edge for comparable aluminum and rock tests. The data recorded for dry Berea sandstone at 400 bars used a lower pass band edge than was used for aluminum at the same pressure. The difference in filter settings is not large (70 vs. 38 kHz) compared to the signal bandwidth. The difference seems to occur at a frequency that is much too low to affect the amplitude spectra. However, the filter has an unknown and possibly significant effect on the phase. For a more

conclusive comparison of the high pressure results the data should be collected using identical filter settings.

Preliminary analysis of S wave phase velocity data was hampered by an apparently greater sensitivity to the filter settings employed in the measurement. No consistent results have been obtained from limited S wave data because sample and reference spectra at comparable pressure and filter parameters are not yet available.

For water saturated samples, Q_{pd} and Q_{pa} are in fairly close agreement at the three pressures. The Q values increase with pressure but are significantly lower than those for the dry samples, and appear to approach a constant value with pressure.

Plots of the amplitude and phase spectra, fits for amplitude spectral ratios, phase velocities, and dispersive Q are shown for the six data sets in Figures 2-28.

Figures 2-7 are plots of the fits of Q determined from amplitude spectral ratios, with pressure and saturation as detailed in figure captions. Data reference numbers are at the top of each figure and are listed in Table 1 for reference.

The lower of the two graphs in each of figures 2-7 plots the amplitude spectrum of the aluminum as a solid line and the amplitude spectrum of the rock as a dashed line. The upper half shows the log of the ratio of rock to

aluminum amplitude spectra. A straight line is fit over the portion of this graph delineated by the vertical bars. Q is calculated from the slope of the line, M, by $M=x/2Qc$, where x is sample length and c is velocity as measured in the laboratory.

Inspection of the plots of amplitude spectral ratios shows that the assumption of constant Q is a reasonable one over the frequency range sampled, as the log of the ratios does not vary greatly from a straight line over the frequency range fit.

Phase velocities as calculated with equation (4.13) are shown in Figures 8-13. Curves for three different values of n are given, and the curve chosen in Q calculations is the one showing the least dispersion over the sampled frequency range. Phase velocity goes to zero for this data at low frequencies effectively since no energy at these frequencies has arrived during the sampled time.

Figures 14-19 illustrate the results when Q is calculated using the appropriate phase velocity data and a reference frequency of 1MHz in equation (4.15). The lower half of each figure shows the chosen dispersion curve with $c(\omega)$ in Kft/sec, along with the rock amplitude spectrum. The upper half plots Q from equation (4.15), in the region where rock amplitude is greater than 25% of the maximum amplitude.

When the phase velocity at any frequency is close to

the reference velocity, the calculated Q values become extremely large. For most of the cases tested, (Figures 16-19), there is a distinct region where the Q is apparently constant. For two cases (Figures 14 and 15) of dry rock at low pressure there is no distinct region of constant Q, and minima have been chosen as determined values. No systematic error analysis justifies this choice, but trials with varying reference frequencies indicate that a lower reference frequency would result in a flat portion of the curve around this minimum. The ambiguity of reference frequencies does not allow a conclusive result for this method.

Only when dispersion is expected to be significant (>1% over the frequency range measured) can calculation of Q by this method be expected to be very useful. However, this includes many of the crustal sedimentary rocks and sediments being explored with various seismic techniques, such as VSP and reflection seismology.

Figures 29-37 are the waveforms analysed. Ideally, both amplitude and phase operators can be developed to produce synthetic waveforms for comparison with the observed pulse shapes, thereby using more of the information contained in the waveform than amplitude or phase alone.

VI. CONCLUSION

Both of the methods used in this paper to evaluate Q, analysis of amplitude spectral ratios and of phase velocity dispersion, give similar results, but the comparison is not consistent for all data. Viscoelastic theory predicts that the two approaches are mathematically equivalent under certain assumptions, so the choice of which is more useful depends upon the application. Where dispersion in the medium under study predominates compared with other sources of dispersion (for example, geometric effects in borehole seismic applications), calculation of phase velocity may reveal attenuation simply.

Comparison of the results presented here with those of Johnston (1978) shows that his Q values for the same sandstone exhibit the same behavior with pressure and saturation but are somewhat higher. Q can vary within a formation due to clay content, and the accuracy of measurement decreases with increasing Q.

Since the various theoretical models predict forms of dispersion-attenuation relations that are quite similar for our purposes, there is no particular model that is favored by the results. Investigation of attenuation over a wider frequency range would be necessary to distinguish among models.

Models assuming constant and near constant Q have been considered for practical purposes, keeping in mind their

potential pitfalls when dealing with real earth data. When measurement of Q in a particular upper crustal region of the earth is the objective, a constant Q approximation gives consistent results. When extrapolating Q over wide frequency ranges or to great earth depths, the approximations break down.

The assumption of constant Q has been made in this analysis. Attenuation varies significantly between different rock types and from varying rock saturation conditions. Some apparent variation from a constant Q value is observed but this does not limit the usefulness of Q as a seismic parameter.

LIST OF SYMBOLS USED IN TEXT

A	=	amplitude
c	=	phase velocity
E	=	energy
$F[\ ]$	=	Fourier Transform
$H[\ ]$	=	Hilbert Transform
$K(\omega)$	=	complex wavenumber
$M(\omega)$	=	complex elastic modulus
Q	=	seismic quality factor
Q_{pa}	=	P-wave Q calculated from amplitude spectral ratios
Q_{pd}	=	P-wave Q calculated from observed phase velocity dispersion
t	=	time
u	=	displacement in one dimension
x	=	sample length, or propagation direction
α	=	attenuation coefficient
γ	=	exponent fit in proposed power law creep function
ε	=	strain
λ	=	wavelength
ρ	=	density
σ	=	stress
Φ	=	relaxation function
ψ	=	creep function
ω	=	angular frequency

ACKNOWLEDGMENTS

I would like to first thank my advisor, Professor Nafi Toksöz, for his continuing support, guidance and encouragement during my stay at MIT.

My work on this thesis was completed only with the gracious assistance of Mark Willis and Karl Coyner. Thanks to Mark for the use of his programs and for his generosity with time given to help and discussions. Thanks to Karl for the use of ultrasonic data collected in his lab.

Others whose help is most appreciated are Darby Dyar, for introducing me to yet another computer, and Steve McDonald, for convincing two computers to talk to each other. A special word of thanks to Ron Marks for help in data transmission, editing, and legwork, not to mention all purpose cheerful moral support.

I'd like to also take this chance to thank all my friends in the Earth and Planetary Science Department at MIT- staff, students, and faculty - for making the department a friendly and supportive work environment.

During part of this work I was supported by a Chevron Fellowship and as an employee of the Chevron Oil Field Research Co., and I acknowledge their help.

REFERENCES

Aki, K., and Richards, P.G., Quantitative Seismology: Theory and Methods, W.H. Freeman and Co., San Francisco, 1980

Azimi, S.A., Kalinan, A.Y.,Kalinan. V.V., and Pivovarov, B.L., Impulse and Transient Characteristics of media with linear and quadratic Absorbtion Laws, Izv. Acad. Sci. USSR Phys. Solid Earth, 1968, 2, p.88-93

Biot, M.A., Theory of Propagation of Elastic Waves in a Fluid-Saturated Porous Solis. II. Higher Frequency Range, Jour. Acoust. Soc. Am., 1956, 28, 179-191.

Bland, D.R., The Theory of Linear Viscoelasticity, Pergamon Press, Oxford, 1960

Brennan, B.J. and Smylie, D.E., Linear Viscoelasticity and Dispersion in Seismic Wave Propagation, Rev. Geophys. and Space Phys., 1981, 19,2,p.233-246

Coyner, K.B., Ph.D. Thesis, in preparation, M.I.T., 1982

Futterman, W.I., Dispersive Body Waves, Jour. Geophys. Res., 1962, 67, p.5279-5291

Ganley, D.C., and Kanasewich, E.R., Measurement of Absorption and Dispersion from Check Shot Surveys, Jour. Geophys. Res., 1980, 85, 5219-5226.

Gardner, G.H.F., Wyllie, M.R.J., and Droschak, D.M., Effects of Pressure and Fluid Saturation on the Attenuation of elastic waves in sands, Jour.Petrol. Tech., 1964, 16, p.189-198

Gordon, R.B., and Davis, L.A., Velocity and Attenuation of Seismic Waves in Imperfectly Elastic Rock, Jour.Geophys. Res., 1968, 73, p. 3917-3935

Johnston, D.H., The attenuation of Seismic Waves in Dry and Saturated Rocks, Ph.D. Thesis, M.I.T., 1978

Kjartansson, E., Constant Q-Wave Propagation and Attenuation, Jour. Geophys. Res., 1979, 84, p. 4737-4748

Knopoff, L., Q, Rev. Geophys. Space Phys., 1964, 2, p. 625-660

Lomnitz, C., Creep Measurements in Igneous Rocks, J. Geol., 1956, 64, p. 473

McDonal, F.J., Angona, F.A., Mills, R.L., Sengbush, R.L., Van Nostrand, R.G., and White, J.E., Attenuation of Shear and Compressional Waves in Pierre Shale, Geophysics, 1958, 23, p. 421-439

Stacey, F.D., Gladwin, M.T., McKavanagh, B., Linde, A.T., and Hastie, L.M., Anelastic Damping of Acoustic and Seismic Pulses, Geophysical Surveys, 1975, 2, p. 133-151

Toksöz, M.N., and Johnston, D.H., eds., Seismic Wave Attenuation, Geophysics reprint series, no.2, 1981

Toksöz, M.N., Johnston, D.H., and Timur, A., Attenuation of Seismic Waves in Dry and Saturated Rocks: I.Laboratory Measurements, Geophysics, 1979, 44, p. 681-690

Tribolet, J.M. A New Phase Unwrapping Algorithm, IEEE Trans. on Acoustics, Speech and Signal Porcessing, 1977, ASSP25, no.2, 170-177

White, J.E., Seismic Waves: Radiation, Transmission, and Attenuation, McGraw-Hill, New York, 1965

Willis, M.E., Ph.D. Thesis, in preparation, M.I.T., 1982

Wuenschel, P.C., Dispersive Body Waves - An Experimental Study, Geophysics, 1965, 30, 539-551

Zamanek, J.Jr., and Rudnick, J., Attenuation and dispersion of elastic waves in a cylindrical bar, Jour. Acoust. Soc. Am., 1961, 33, p. 1283-1288

Table 1

DRY BEREA SANDSTONE

pressure (bars)	Q_{pd}	Q_{pa}	Vp (ft/sec)	Data reference no.
100	22	25	11272	BR1118.2A
250	45	46	12810	BR1118.5A
400	35	74	13244	BR1118.7A

WATER SATURATED BEREA SANDSTONE

*pressure (bars)	Q_{pd}	Q_{pa}	Vp (ft/sec)	Data reference no.
100	15	16	12805	BR1122.5B
250	30	30	13330	BR1124.8B
400	27	32	13588	BR1210.10B

* differential pressure, fluid pressure in all saturated cases is 100 bars.

FIGURE CAPTIONS

Figure 1. Summary of results of Q calculations. Q calculated from amplitude spectral ratios of P waves is referred to as Q_{pa}. Q calculated from P-wave phase velocity dispersion is referred to as Q_{pd}.

Figures 2-7. Berea Sandstone. Amplitude spectra and spectral ratios, showing Q fits. Lower half is plot of the two amplitude spectra, aluminum(solid line) and rock(dashed line). Upper half of each figure is a plot of the log of amplitude ratios. Vertical bars delineate portion of upper graph used to fit slope M. V is velocity measured in lab. Key to data reference numbers at top of each figure is given in Table 1.

Figure 2. pressure 100 bars, dry rock

Figure 3. pressure 250 bars, dry rock

Figure 4. pressure 400 bars, dry rock

Figure 5. pressure 100 bars, water saturated rock

Figure 6. pressure 250 bars, water saturated rock

Figure 7. pressure 400 bars, water saturated rock

Figures 8-13. Phase velocity(Kft/sec) vs. frequency(KHz). Shown are phase velocities for three different values of the constant n. The curve with the least dispersion in the frequency range corresponding to the energy in the wave is

chosen from these to calculate Q.

Figure 8. pressure 100 bars, dry rock

Figure 9. pressure 250 bars, dry rock

Figure 10. pressure 400 bars, dry rock

Figure 11. pressure 100 bars, water saturated rock

Figure 12. pressure 250 bars, water saturated rock

Figure 13. pressure 400 bars, water saturated rock

Figures 14-19. c(Kft/sec), , amplitude, and Q_d vs. frequency. Lower half plots the dispersion curve used, and amplitude spectrum of rock. Upper half plots Q calculated from equation (4.15) for region around amplitude maximum.

Figure 14. pressure 100 bars, dry rock

Figure 15. pressure 250 bars, dry rock

Figure 16. pressure 400 bars, dry rock

Figure 17. pressure 100 bars, water saturated rock

Figure 18. pressure 250 bars, water saturated rock

Figure 19. pressure 400 bars, water saturated rock

Figures 20-28. Amplitude and phase spectra of waveforms. Phase is in radians.

Figure 20. pressure 100 bars, aluminum

Figure 21. pressure 250 bars, aluminum

Figure 22. pressure 400 bars, aluminum

Figure 23. pressure 100 bars, dry rock

Figure 24. pressure 250 bars, dry rock

Figure 25. pressure 400 bars, dry rock

Figure 26. pressure 100 bars, water saturated rock

Figure 27. pressure 250 bars, water saturated rock

Figure 28. pressure 400 bars, water saturated rock

Figures 29-37. Windowed waveforms. Time in microseconds.

Figure 29. pressure 100 bars, aluminum

Figure 30. pressure 250 bars, aluminum

Figure 31. pressure 400 bars, aluminum

Figure 32. pressure 100 bars, dry rock

Figure 33. pressure 250 bars, dry rock

Figure 34. pressure 400 bars, dry rock

Figure 35. pressure 100 bars, water saturated rock

Figure 36. pressure 250 bars, water saturated rock

Figure 37. pressure 400 bars, water saturated rock

Figure 1

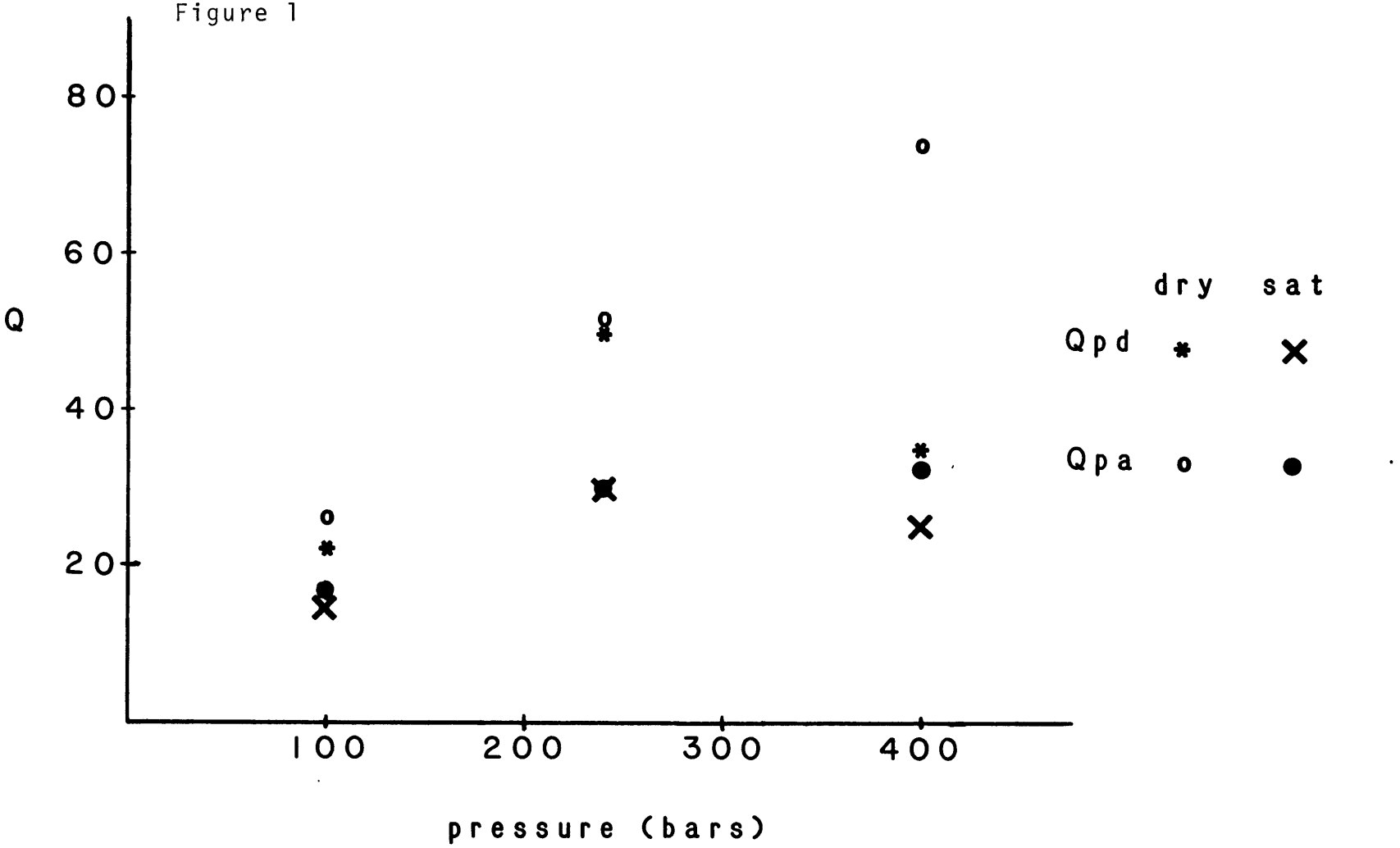

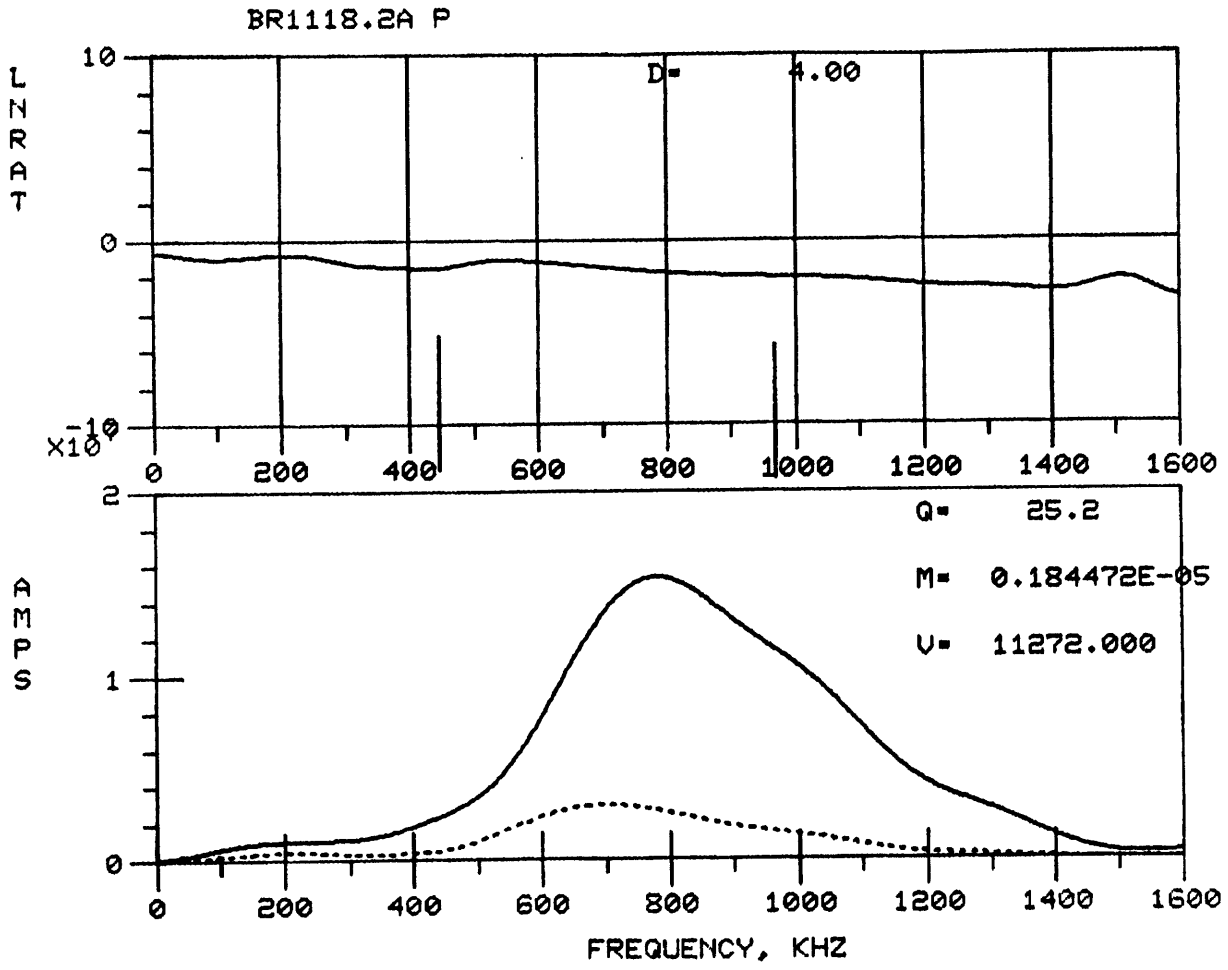
BR1118.2A P
D= 4.00
TRANSMISSION
10
0
-10
X10
0
200
400
600
800
1000
1200
1400
1600
SPMA
2
1
0
Q= 25.2
M= 0.184472E-05
V= 11272.000
FREQUENCY, KHZ

Figure 2

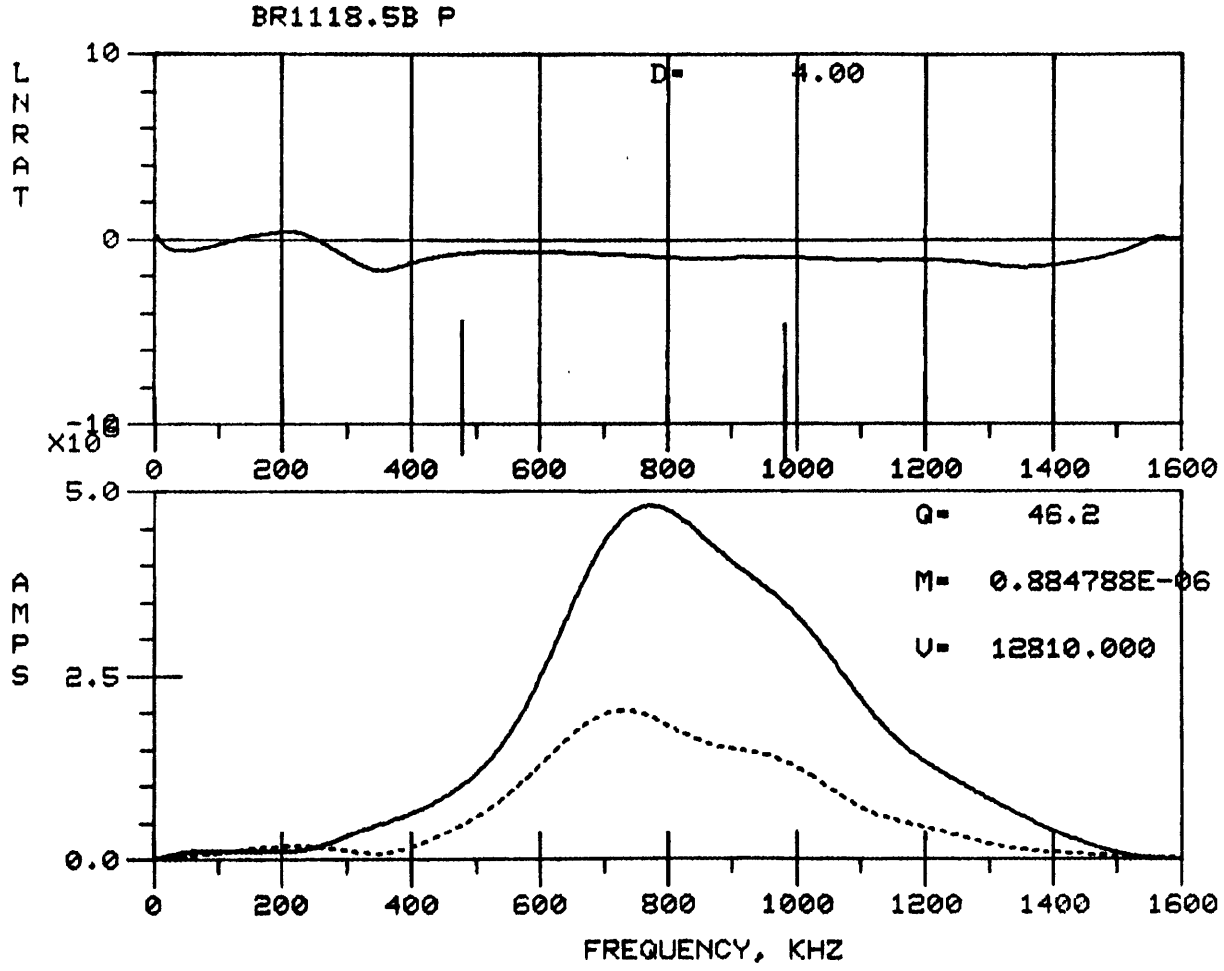
BR1118.5B P
D= 4.00
LNRAT
10
0
-10
X10
0
200
400
600
800
1000
1200
1400
1600
AMPS
5.0
2.5
0.0
Q= 46.2
M= 0.884788E-06
V= 12810.000
FREQUENCY, KHZ

Figure 3

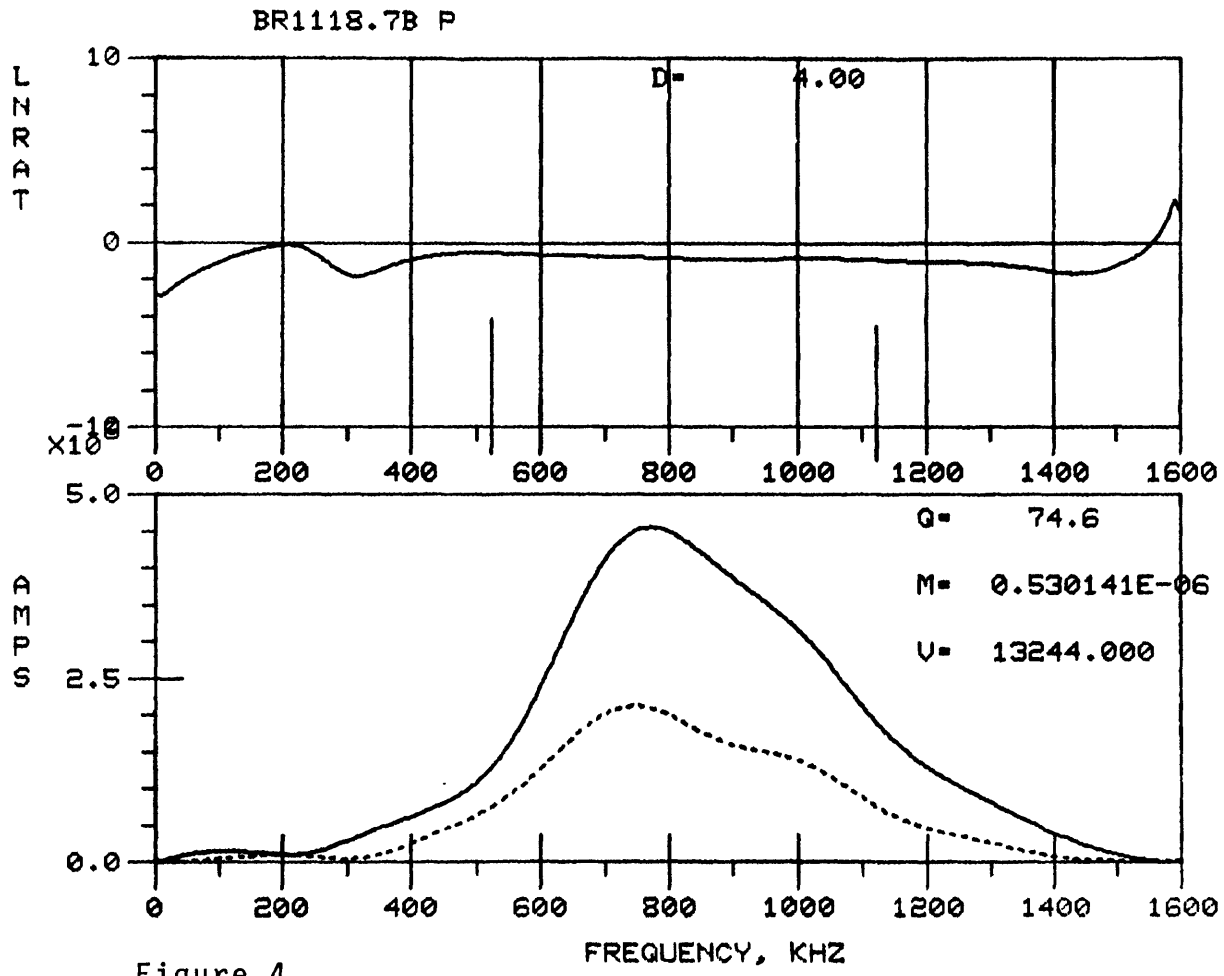
BR1118.7B P
D= 4.00
TANZL
10
0
-10
X10
0
200
400
600
800
1000
1200
1400
1600
5.0
2.5
0.0
AMPS
Q= 74.6
M= 0.530141E-06
V= 13244.000
FREQUENCY, KHZ

Figure 4

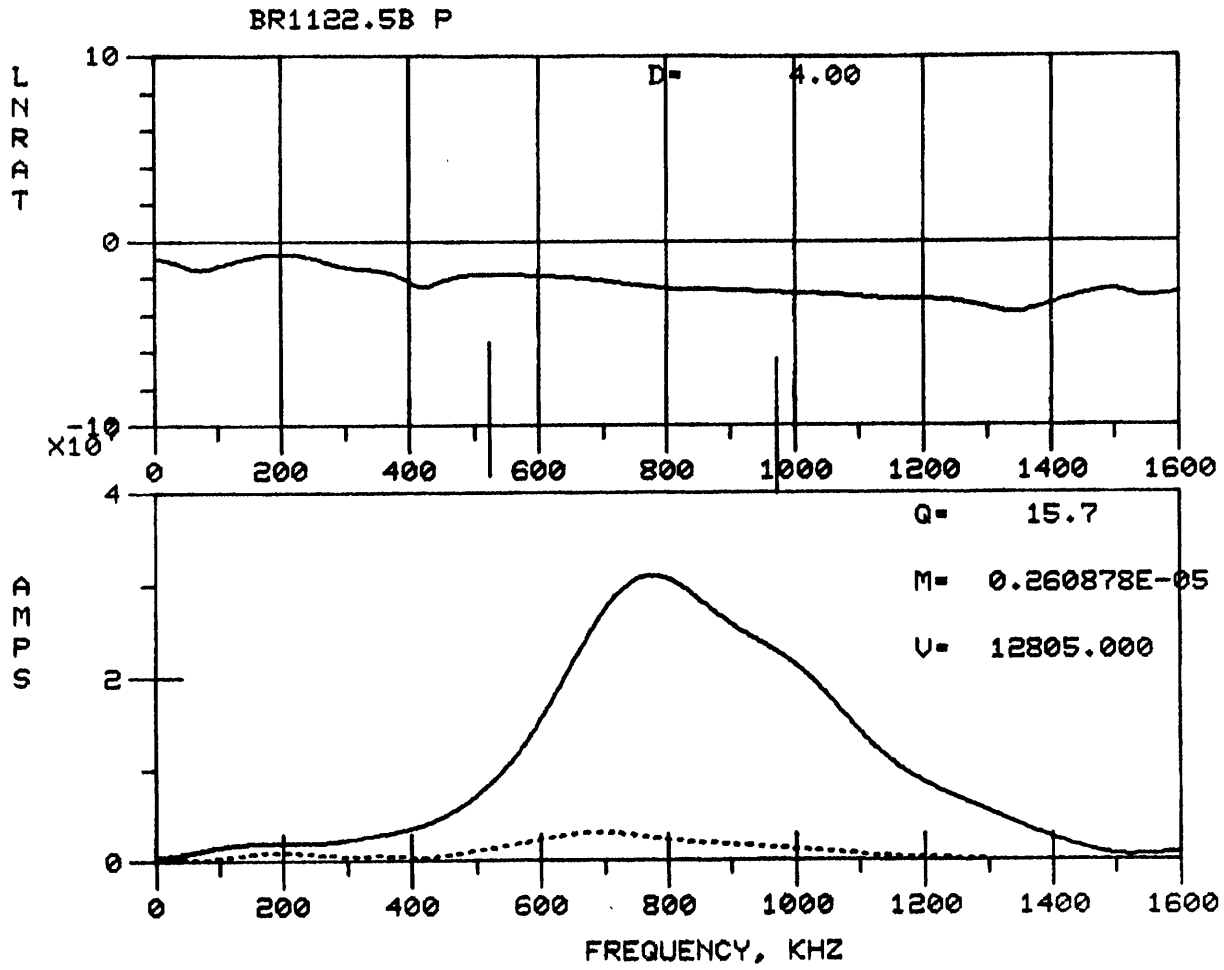
BR1122.5B P
D= 4.00
TANZ
10
0
-10
X10
0
200
400
600
800
1000
1200
1400
1600
AMPS
4
2
0
Q= 15.7
M= 0.260878E-05
V= 12805.000
FREQUENCY, KHZ

Figure 5

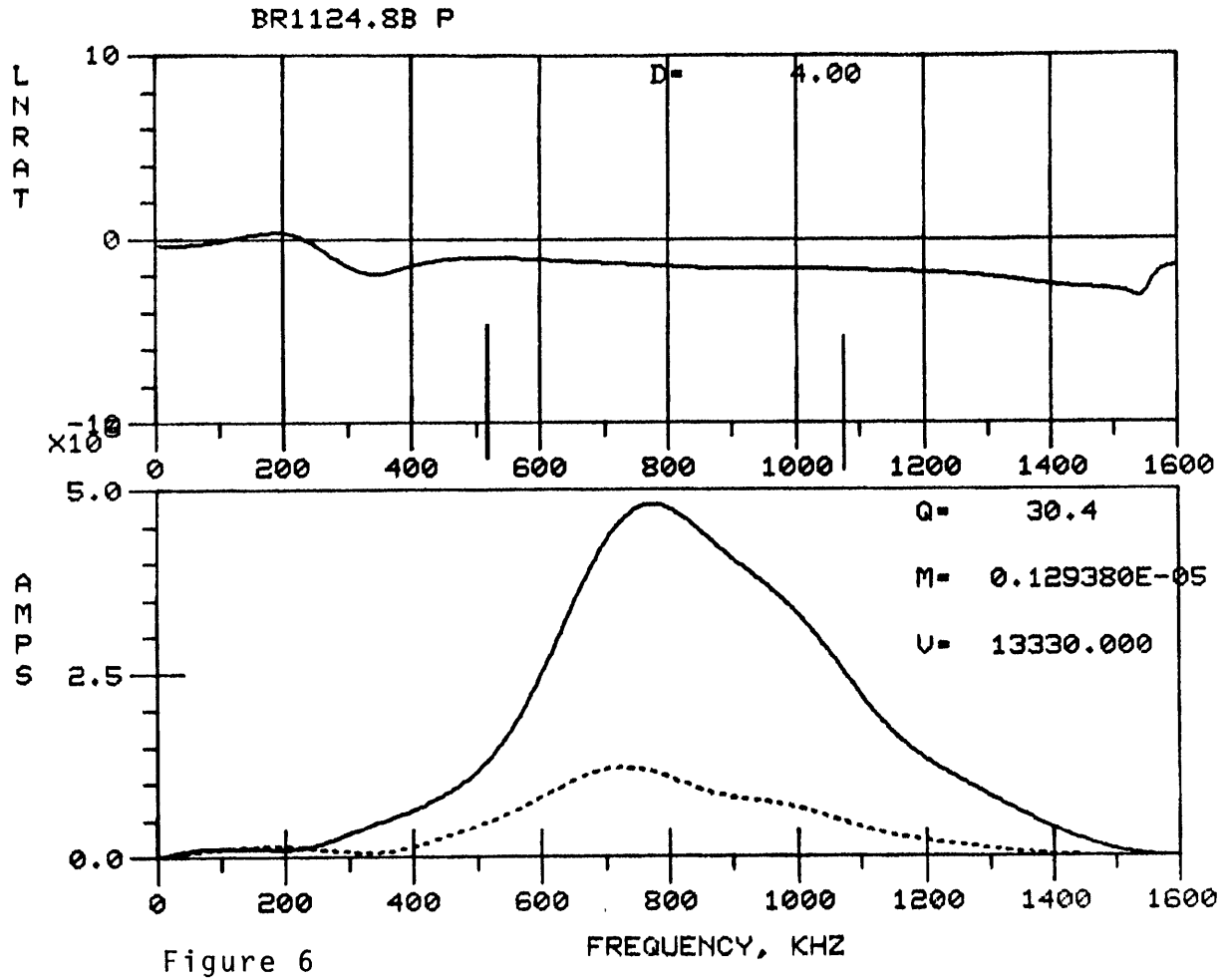
BR1124.8B P
D= 4.00
TRANL
10
0
-10
X10
0
200
400
600
800
1000
1200
1400
1600
SPMA
5.0
2.5
0.0
Q= 30.4
M= 0.129380E-05
V= 13330.000
FREQUENCY, KHZ

Figure 6

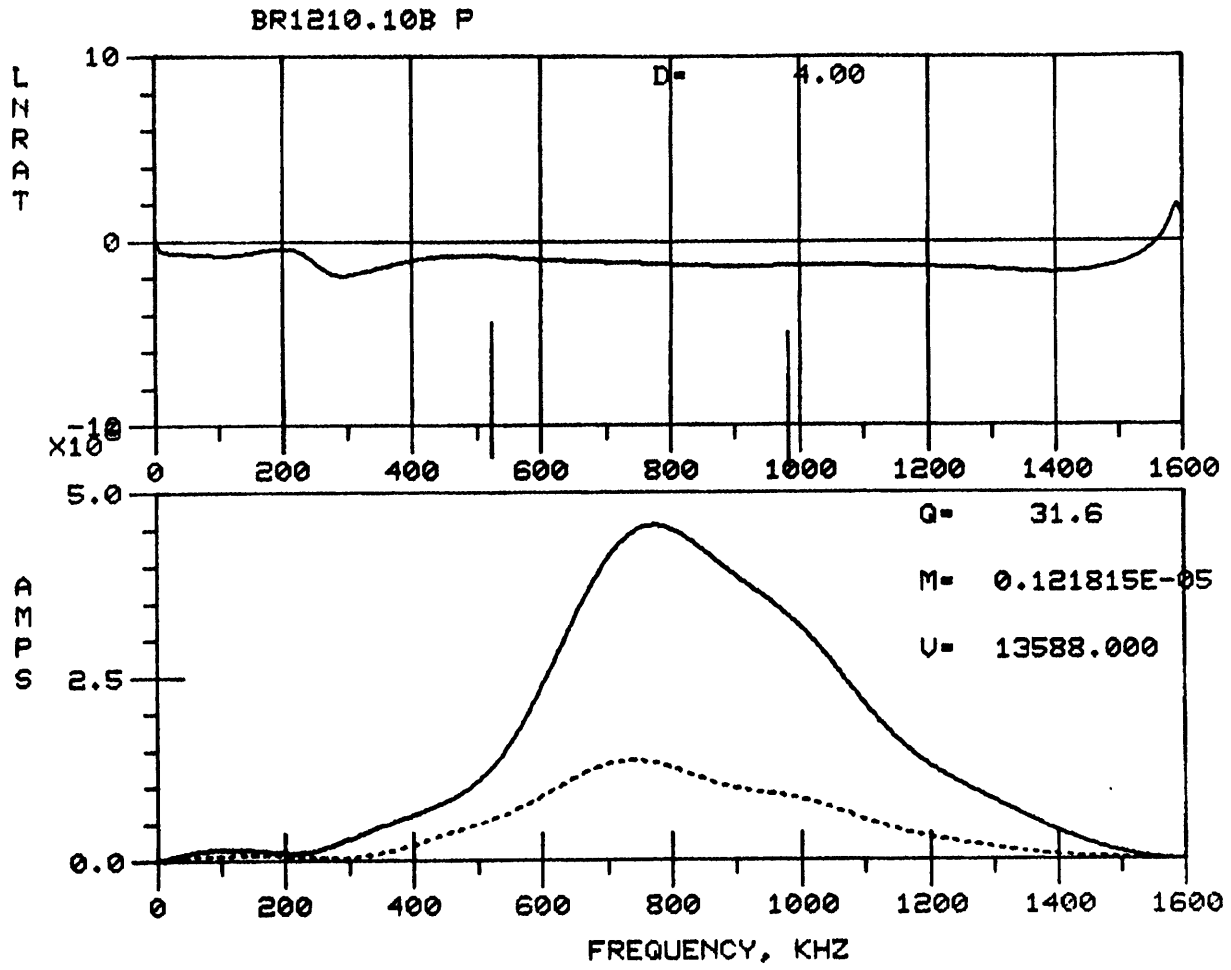
BR1210.10B P
D= 4.00
10
0
-10
X10
0
200
400
600
800
1000
1200
1400
1600
5.0
2.5
0.0
Q= 31.6
M= 0.121815E-05
V= 13588.000
FREQUENCY, KHZ

Figure 7

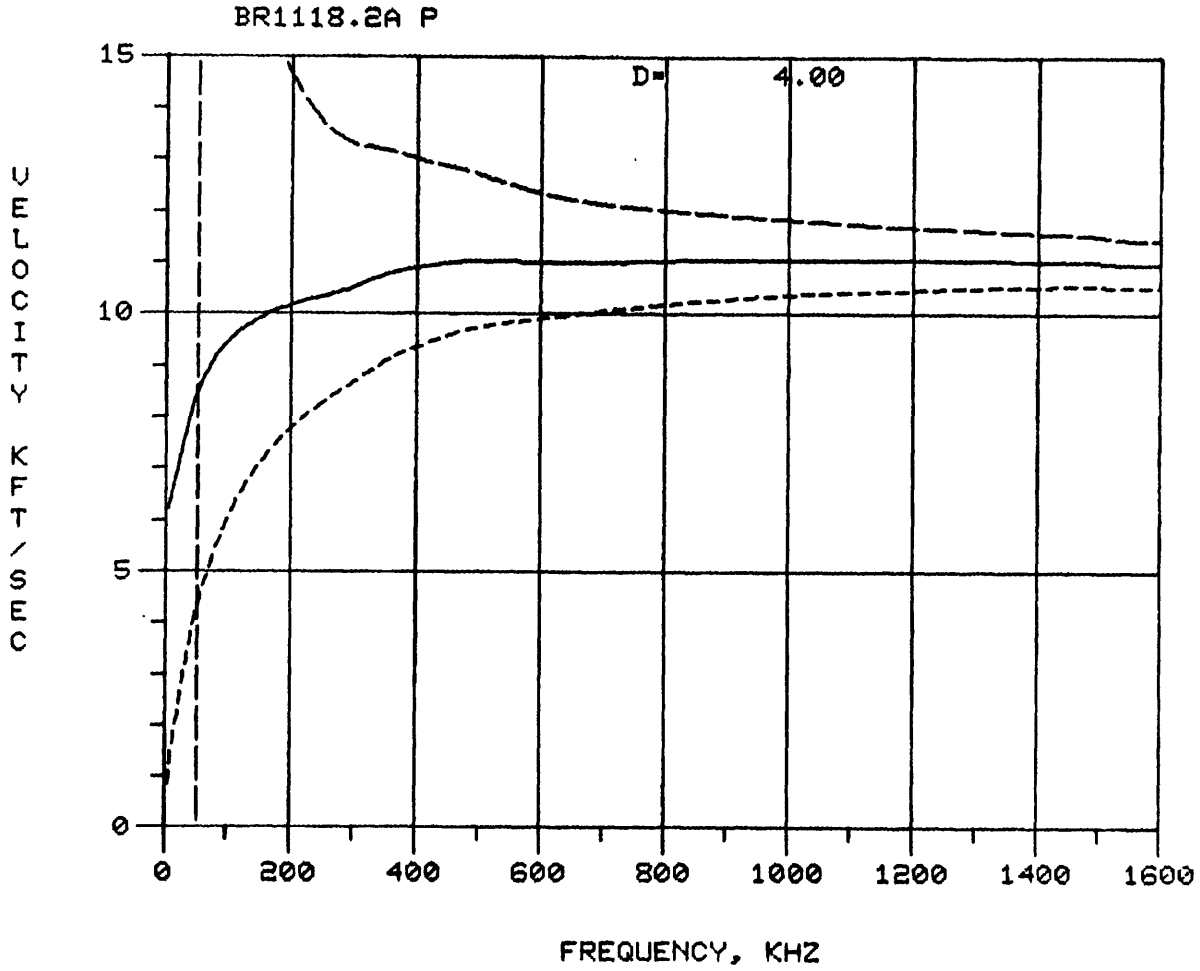
BR1118.2A P
D= 4.00
15
10
5
0
0
200
400
600
800
1000
1200
1400
1600
VELOCITY KFT\SEC
FREQUENCY, KHZ

Figure 8

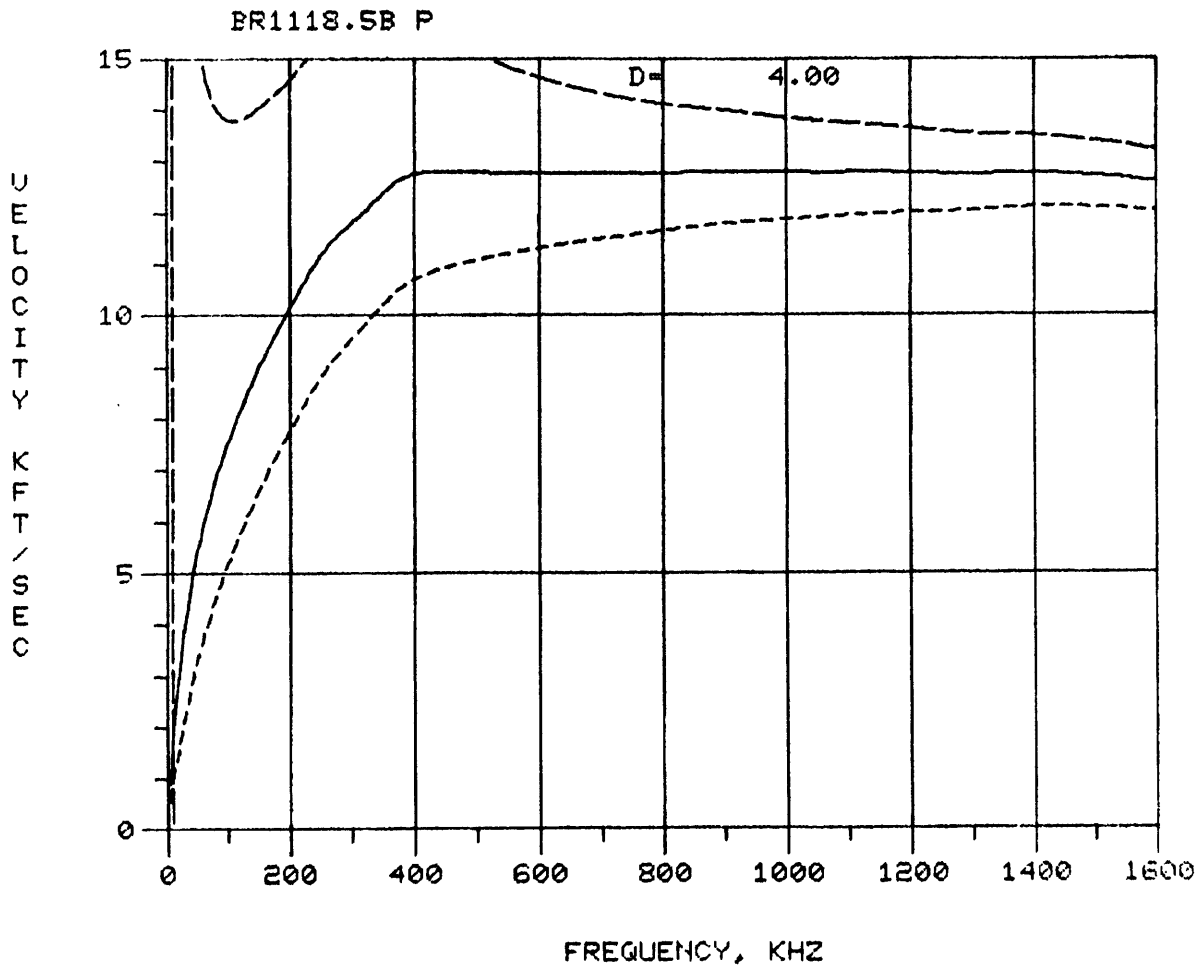
BR1118.SB P
D= 4.00
VELOCITY KFT/SEC
15
10
5
0
0
200
400
600
800
1000
1200
1400
1600
FREQUENCY, KHZ

Figure 9

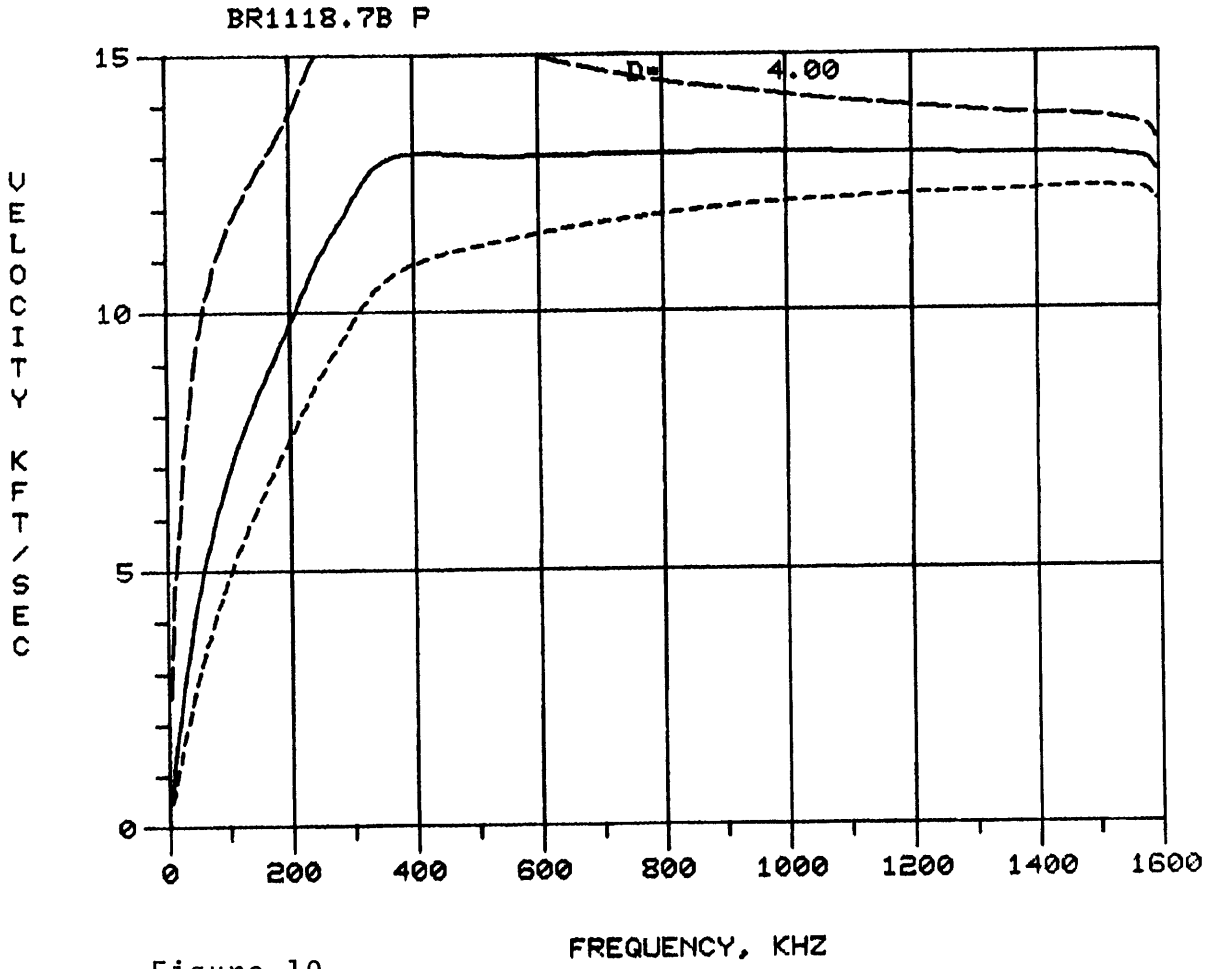
BR1118.7B P
D= 4.00
15
10
5
0
0
200
400
600
800
1000
1200
1400
1600
VELOCITY KFT\SEC
FREQUENCY, KHZ

Figure 10

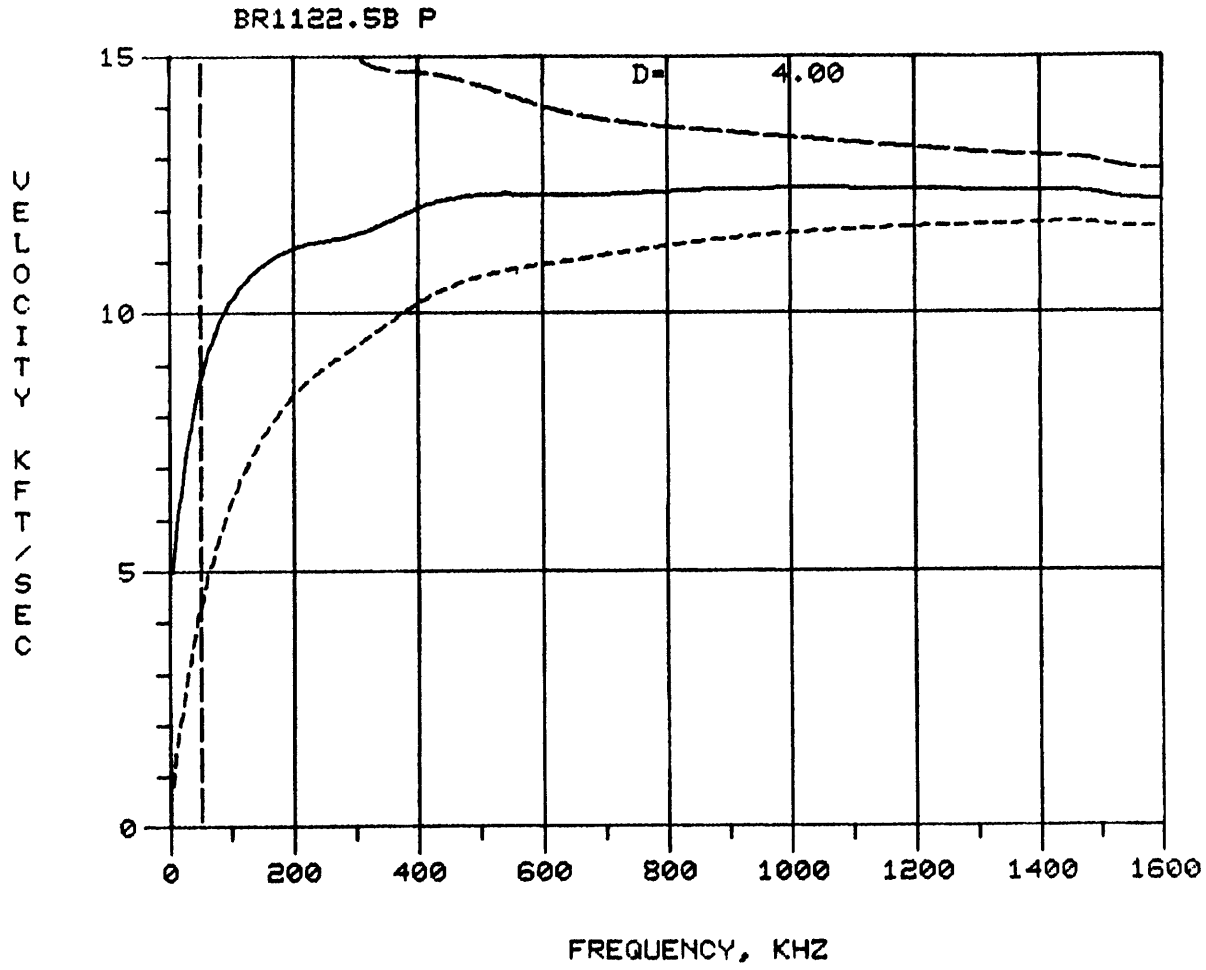
BR1122.5B P
D= 4.00
VELOCITY KFT\SEC
15
10
5
0
0
200
400
600
800
1000
1200
1400
1600
FREQUENCY, KHZ

Figure 11

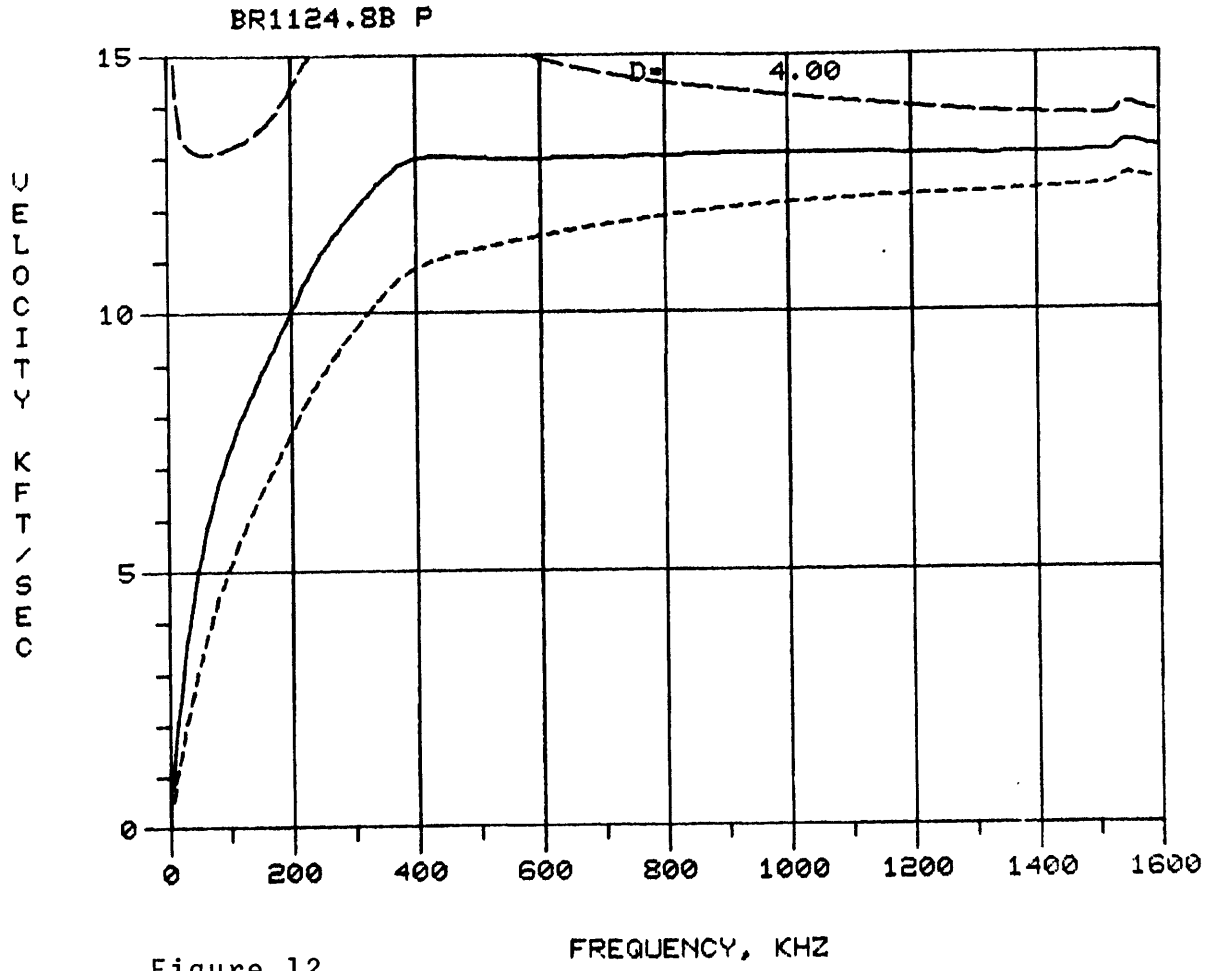
BR1124.8B P
D= 4.00
15
10
5
0
0
200
400
600
800
1000
1200
1400
1600
VELOCITY KFT/SEC
FREQUENCY, KHZ

Figure 12

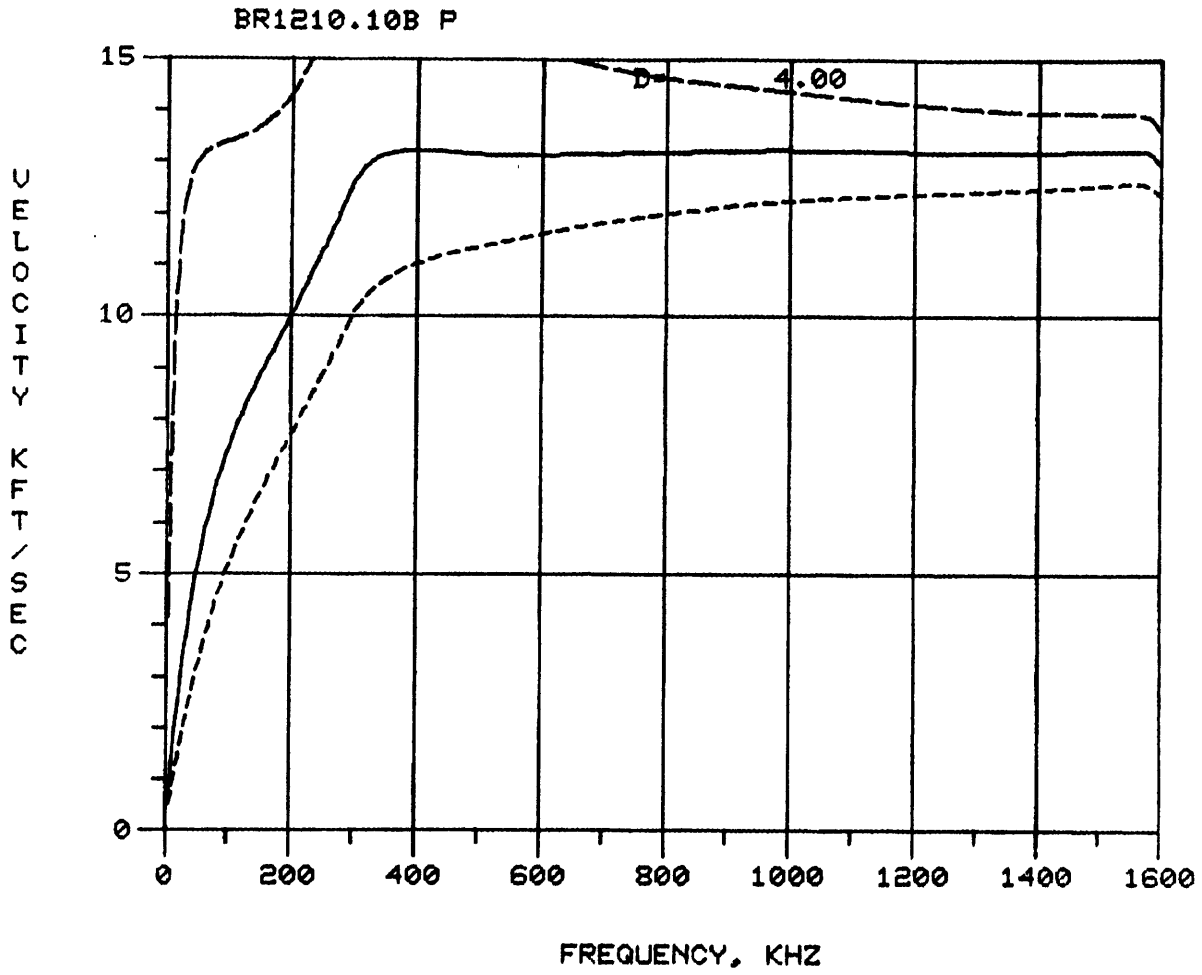
BR1210.10B P
D= 4.00
15
10
5
0
VELOCITY KFT/SEC
0
200
400
600
800
1000
1200
1400
1600
FREQUENCY, KHZ

Figure 13

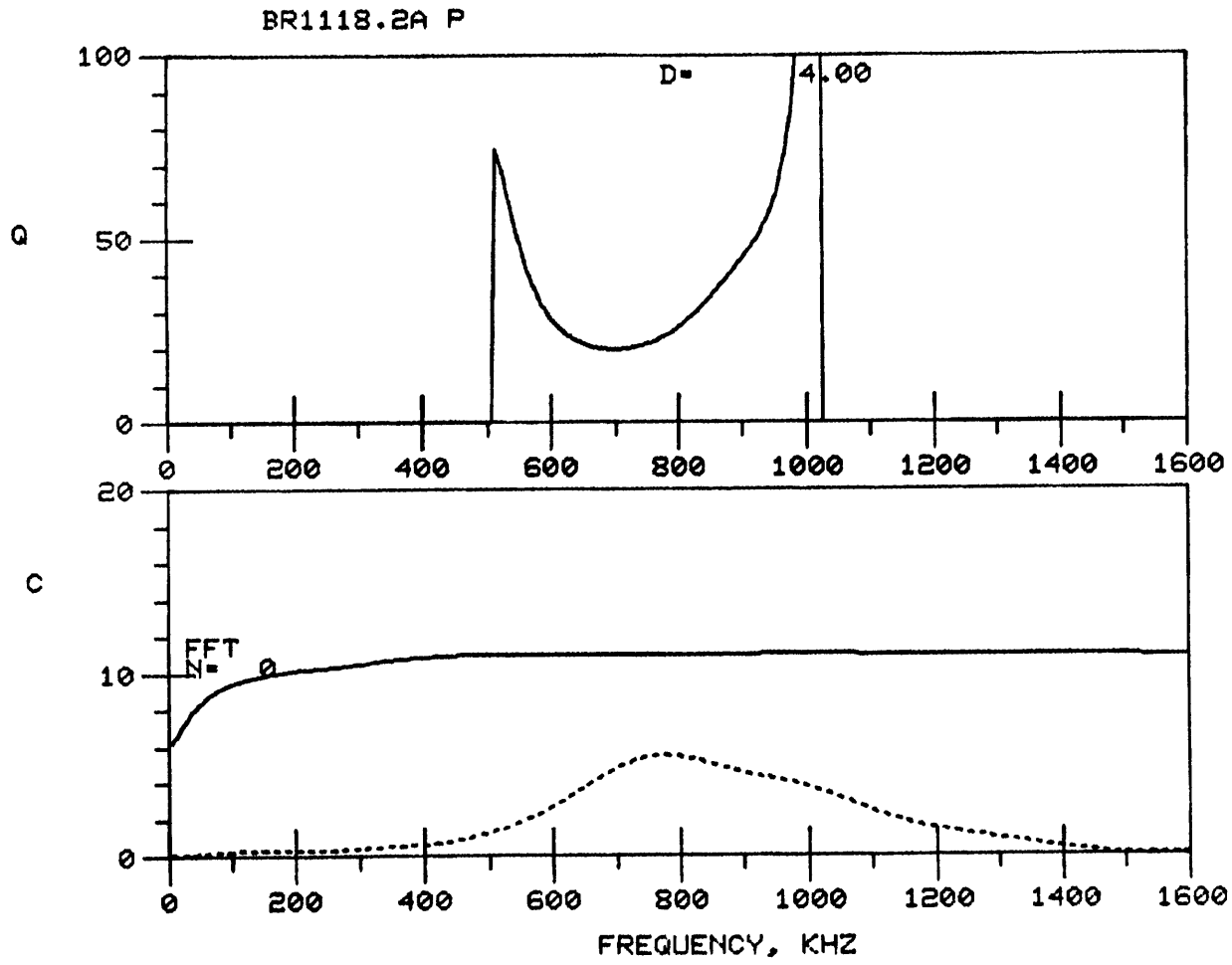
BR1118.2A P
D=
4.00
Q
100
50
0
0
200
400
600
800
1000
1200
1400
1600
C
20
10
0
FFT
N=
0
FREQUENCY, KHZ

Figure 14

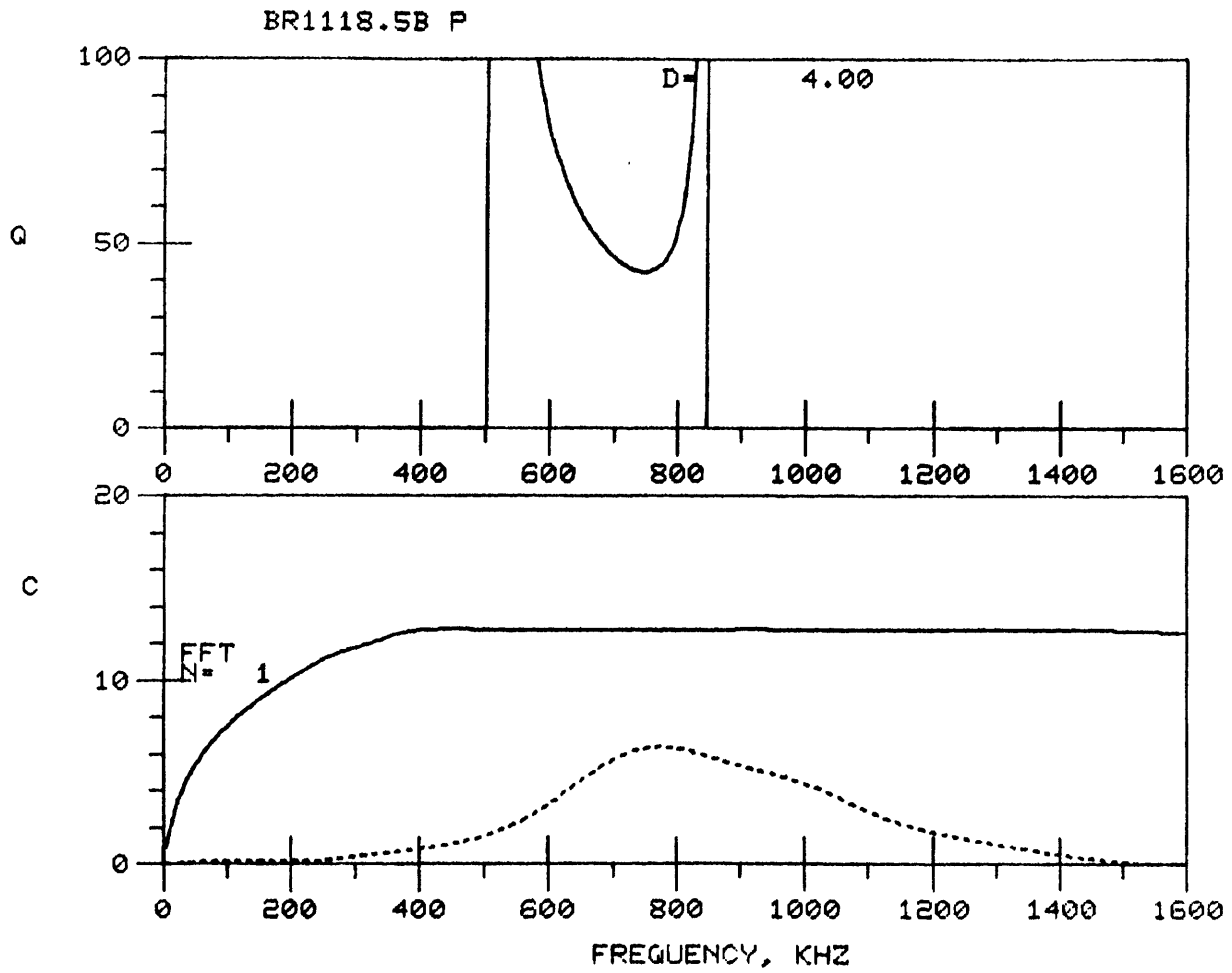
BR1118.5B P
100
50
0
Q
D=
4.00
0
200
400
600
800
1000
1200
1400
1600
20
10
0
C
FFT
N= 1
FREQUENCY, KHZ

Figure 15

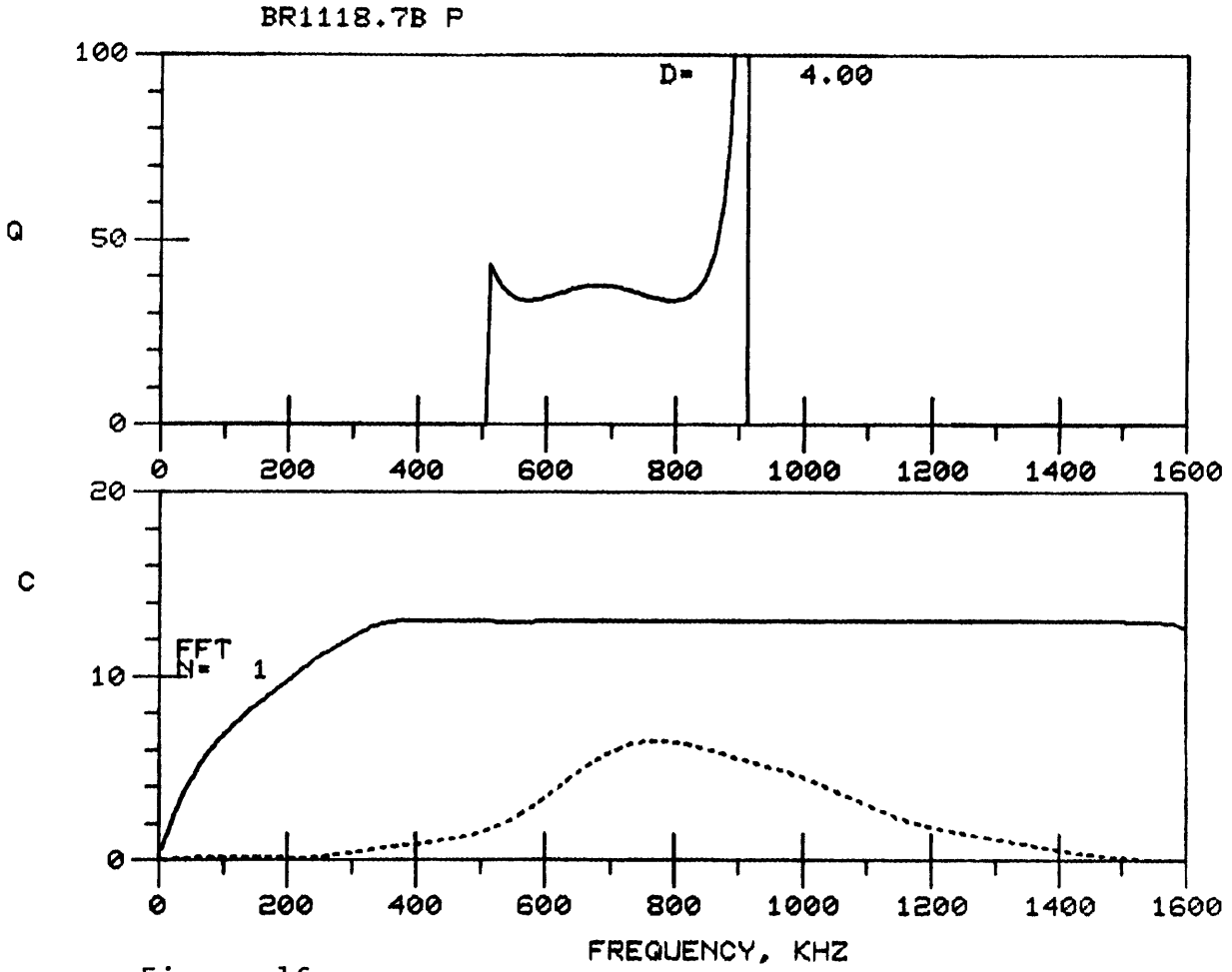
BR1118.7B P
D= 4.00
Q
100
50
0
0
200
400
600
800
1000
1200
1400
1600
C
20
10
0
FFT
N= 1
FREQUENCY, KHZ

Figure 16

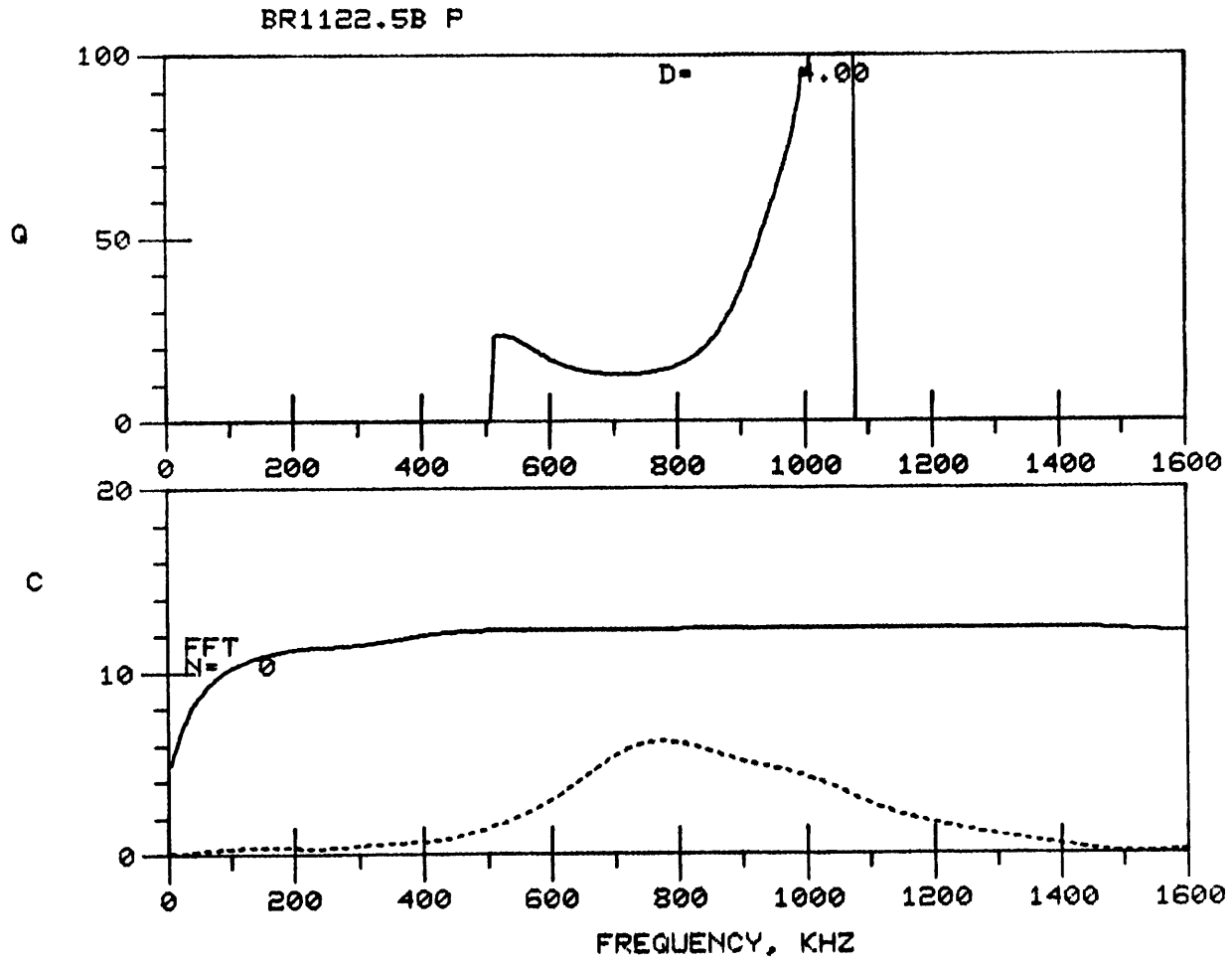
BR1122.5B P
D=
4.00
Q
100
50
0
0
200
400
600
800
1000
1200
1400
1600
C
20
10
0
FFT
N=
0
FREQUENCY, KHZ

Figure 17

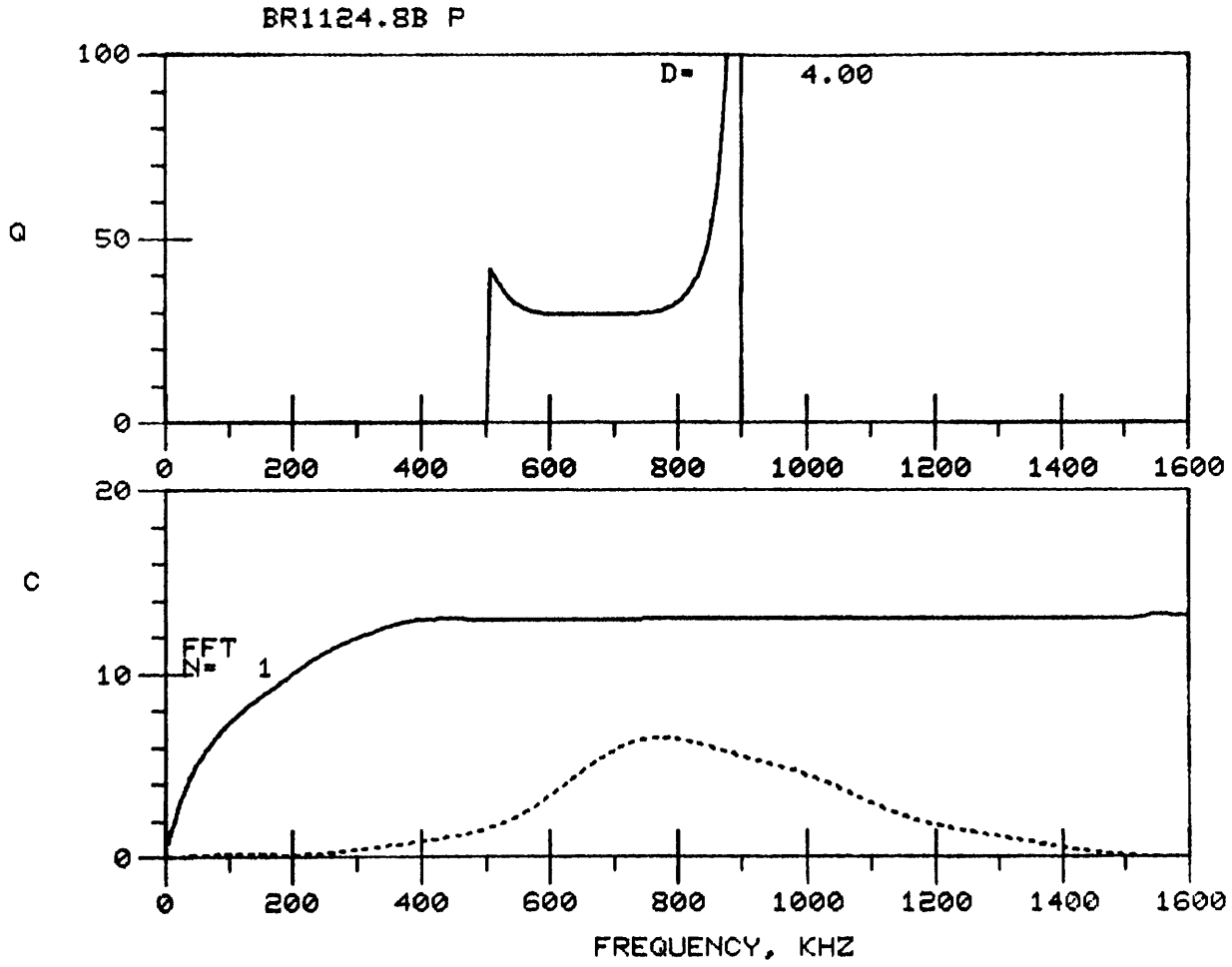
BR1124.8B P
100
50
0
Q
D=
4.00
0
200
400
600
800
1000
1200
1400
1600
20
10
0
C
FFT
N= 1
FREQUENCY, KHZ

Figure 18

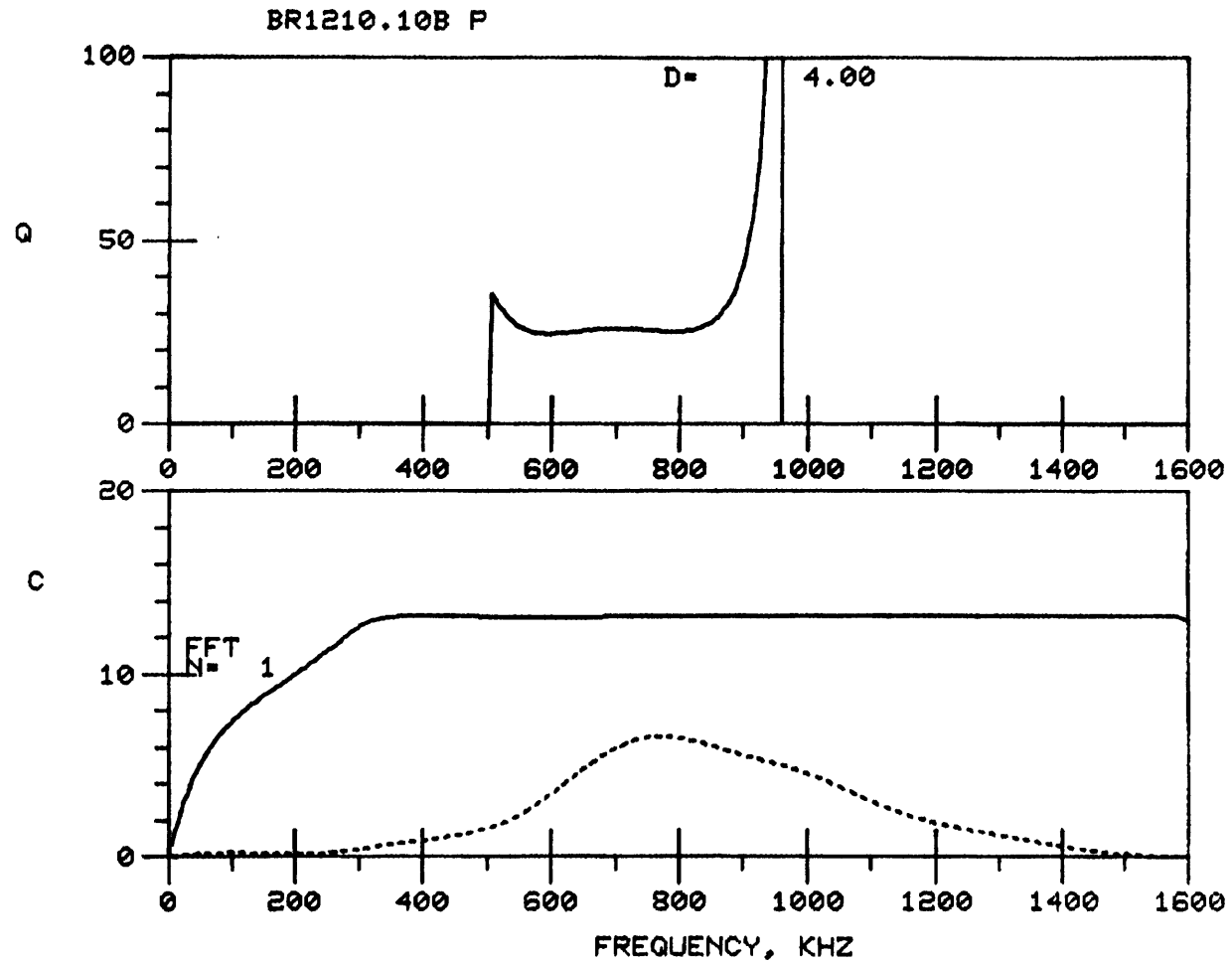
BR1210.10B P
100
50
0
Q
D=
4.00
0
200
400
600
800
1000
1200
1400
1600
20
10
0
C
FFT
N= 1
FREQUENCY, KHZ

Figure 19

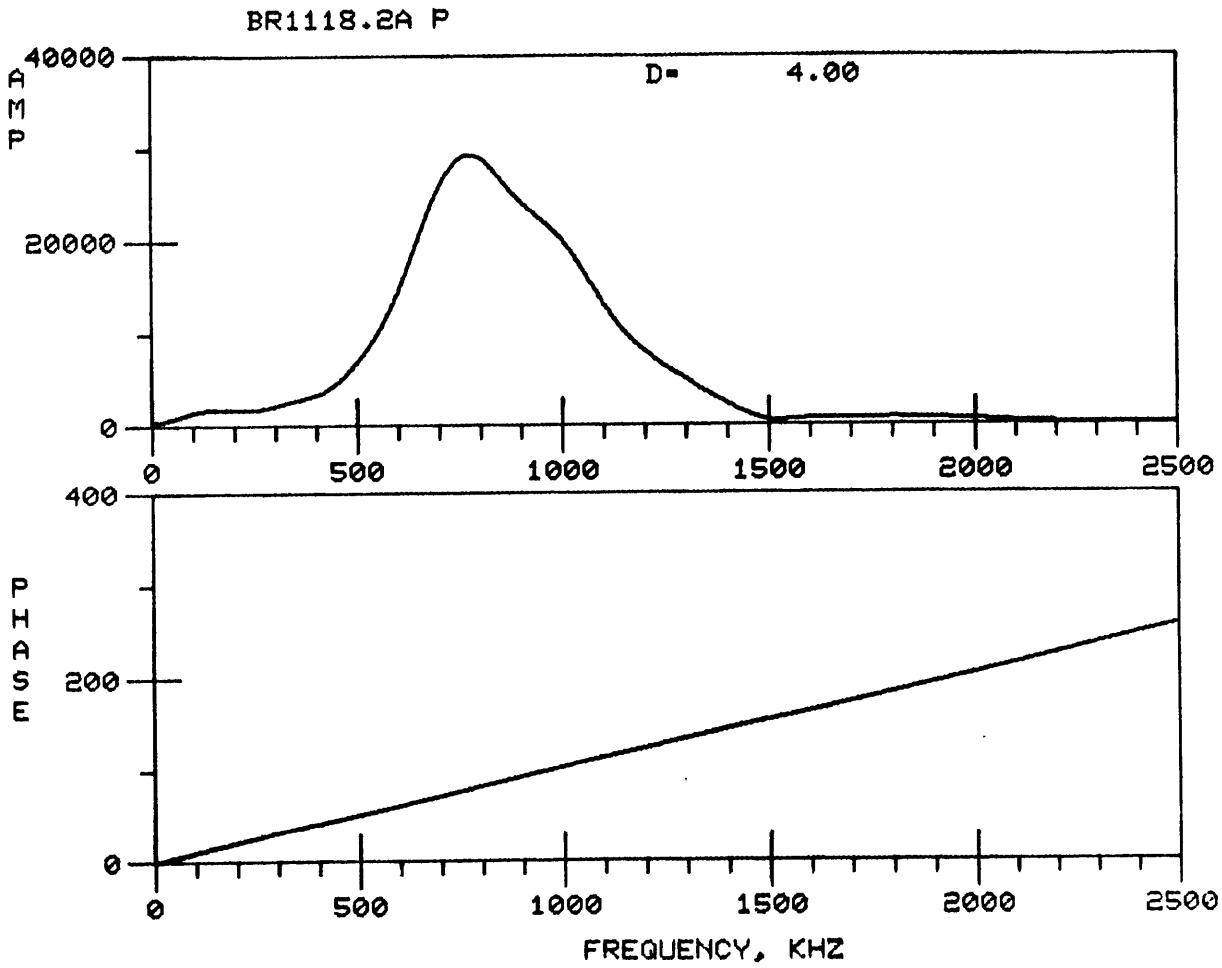
BR1118.2A P
D= 4.00
AMP
40000
20000
0
0
500
1000
1500
2000
2500
PHASE
400
200
0
0
500
1000
1500
2000
2500
FREQUENCY, KHZ

Figure 20

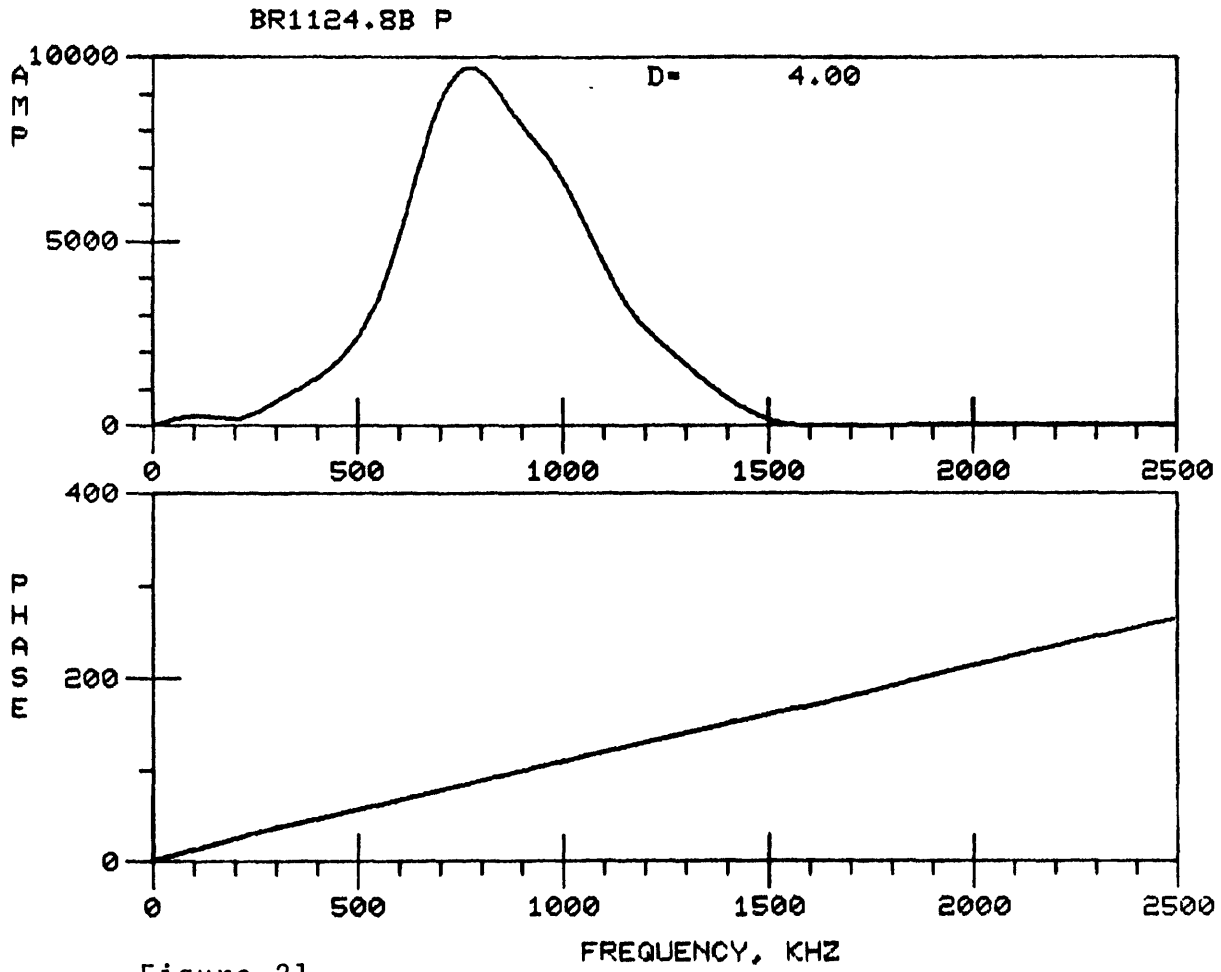
BR1124.8B P
D= 4.00
AMP
10000
5000
0
0
500
1000
1500
2000
2500
PHASE
400
200
0
0
500
1000
1500
2000
2500
FREQUENCY, KHZ

Figure 21

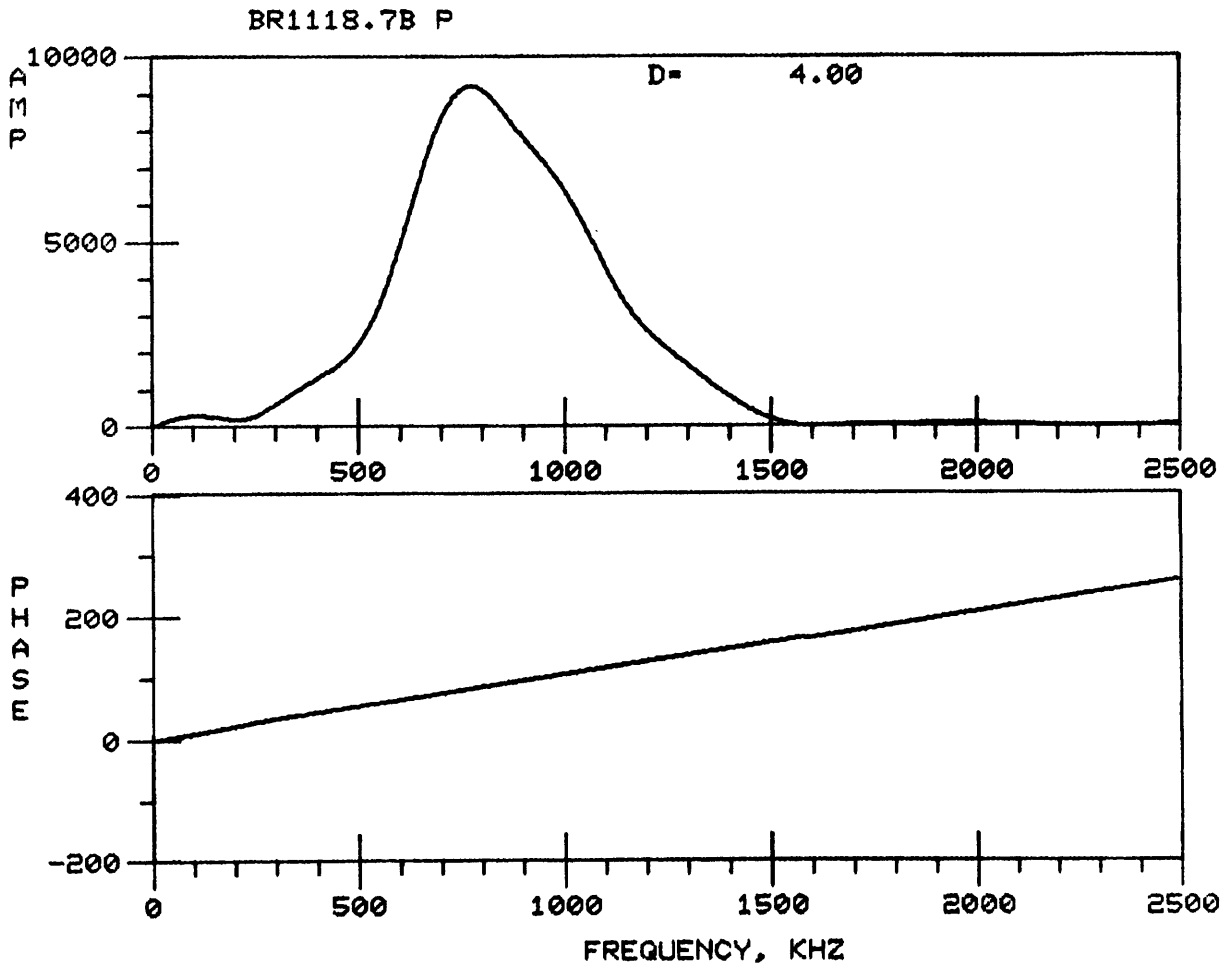
BR1118.7B P
D= 4.00
AMP
10000
5000
0
0
500
1000
1500
2000
2500
PHASE
400
200
0
-200
0
500
1000
1500
2000
2500
FREQUENCY, KHZ

Figure 22

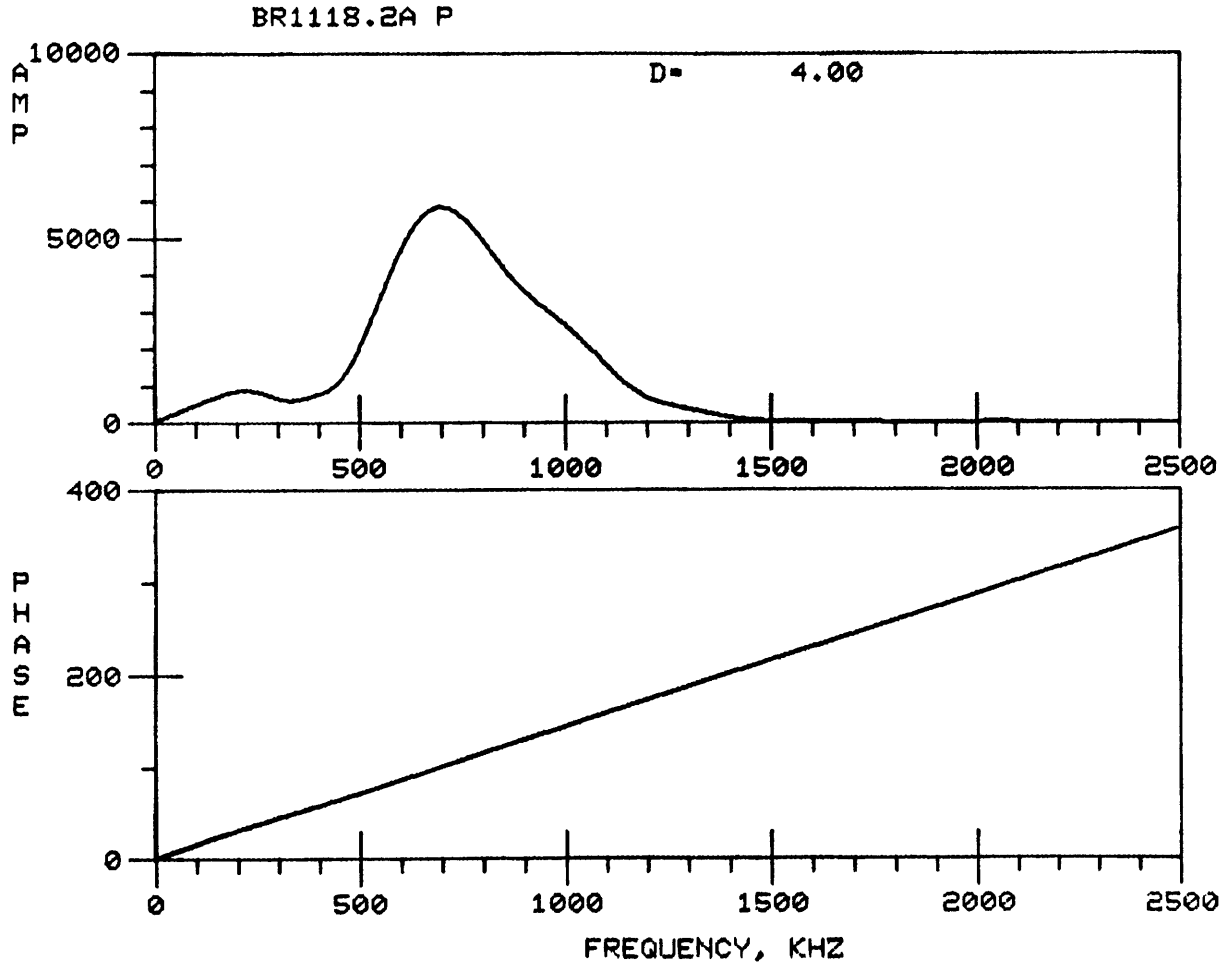
BR1118.2A P
D= 4.00
AMP
10000
5000
0
0
500
1000
1500
2000
2500
PHASE
400
200
0
0
500
1000
1500
2000
2500
FREQUENCY, KHZ

Figure 23

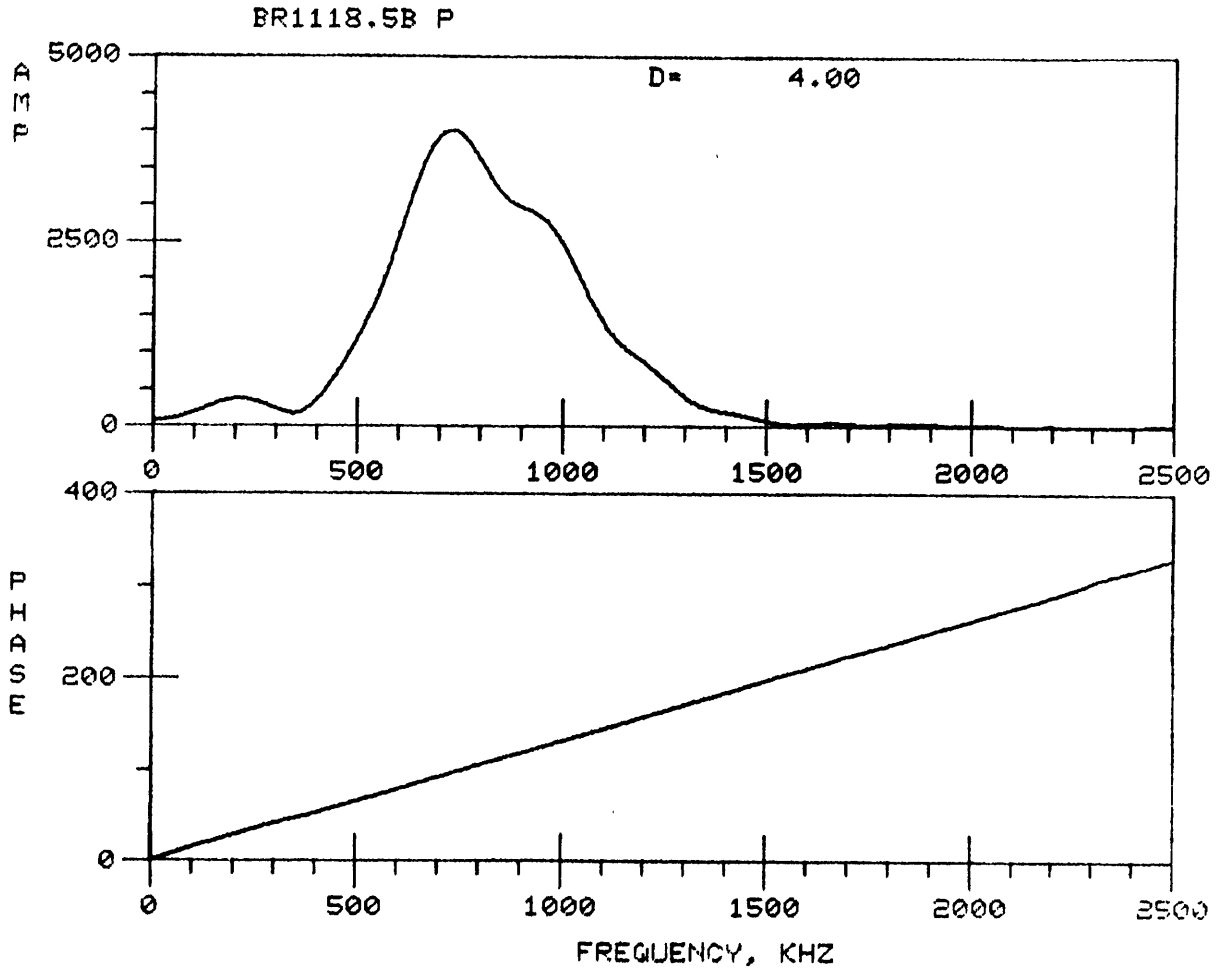
BR1118.5B P
D= 4.00
AMP
5000
2500
0
0
500
1000
1500
2000
2500
PHASE
400
200
0
0
500
1000
1500
2000
2500
FREQUENCY, KHZ

Figure 24

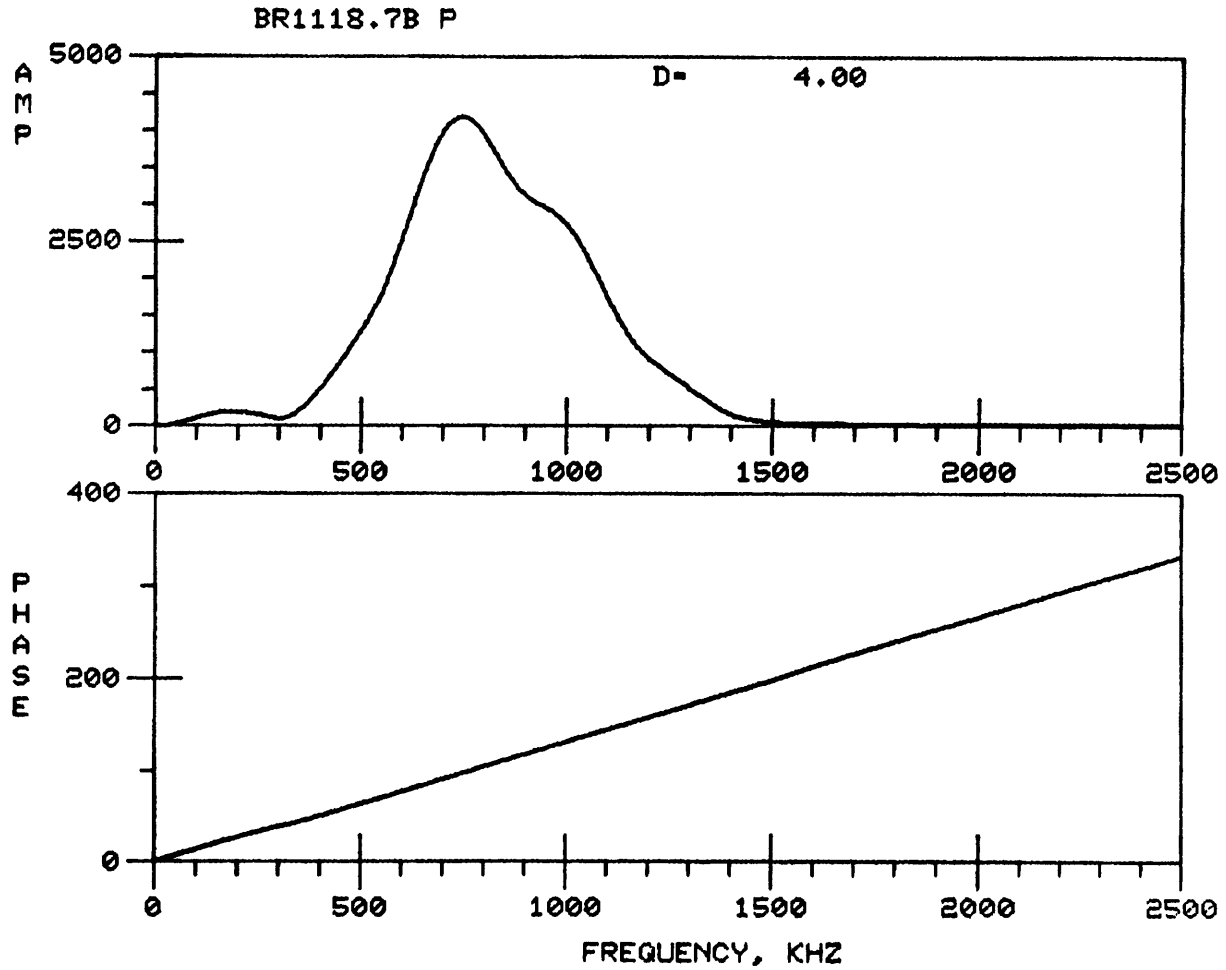
BR1118.7B P
D= 4.00
AMP
5000
2500
0
0
500
1000
1500
2000
2500
PHASE
400
200
0
0
500
1000
1500
2000
2500
FREQUENCY, KHZ

Figure 25

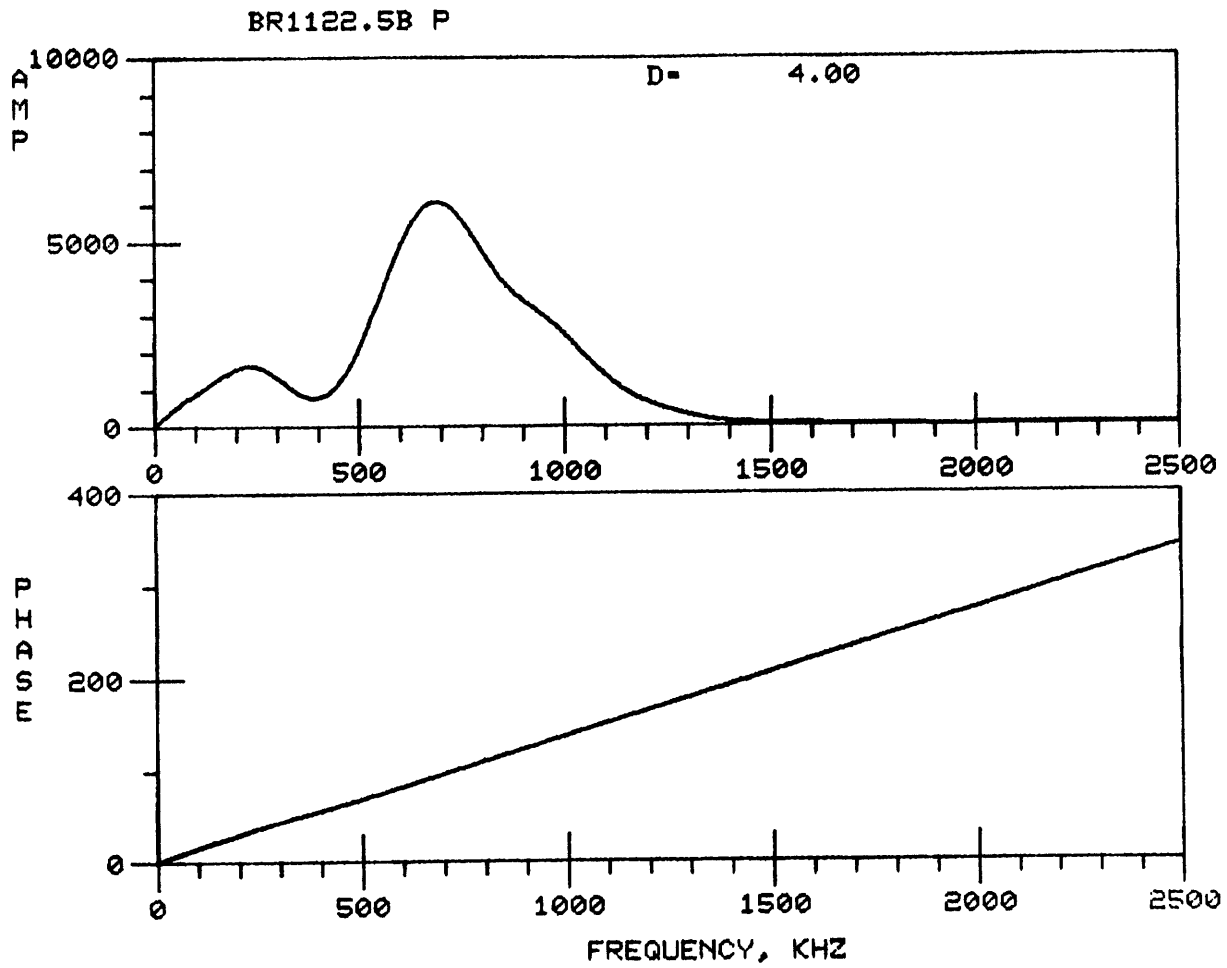
BR1122.5B P
D= 4.00
AMP
10000
5000
0
0
500
1000
1500
2000
2500
PHASE
400
200
0
0
500
1000
1500
2000
2500
FREQUENCY, KHZ

Figure 26

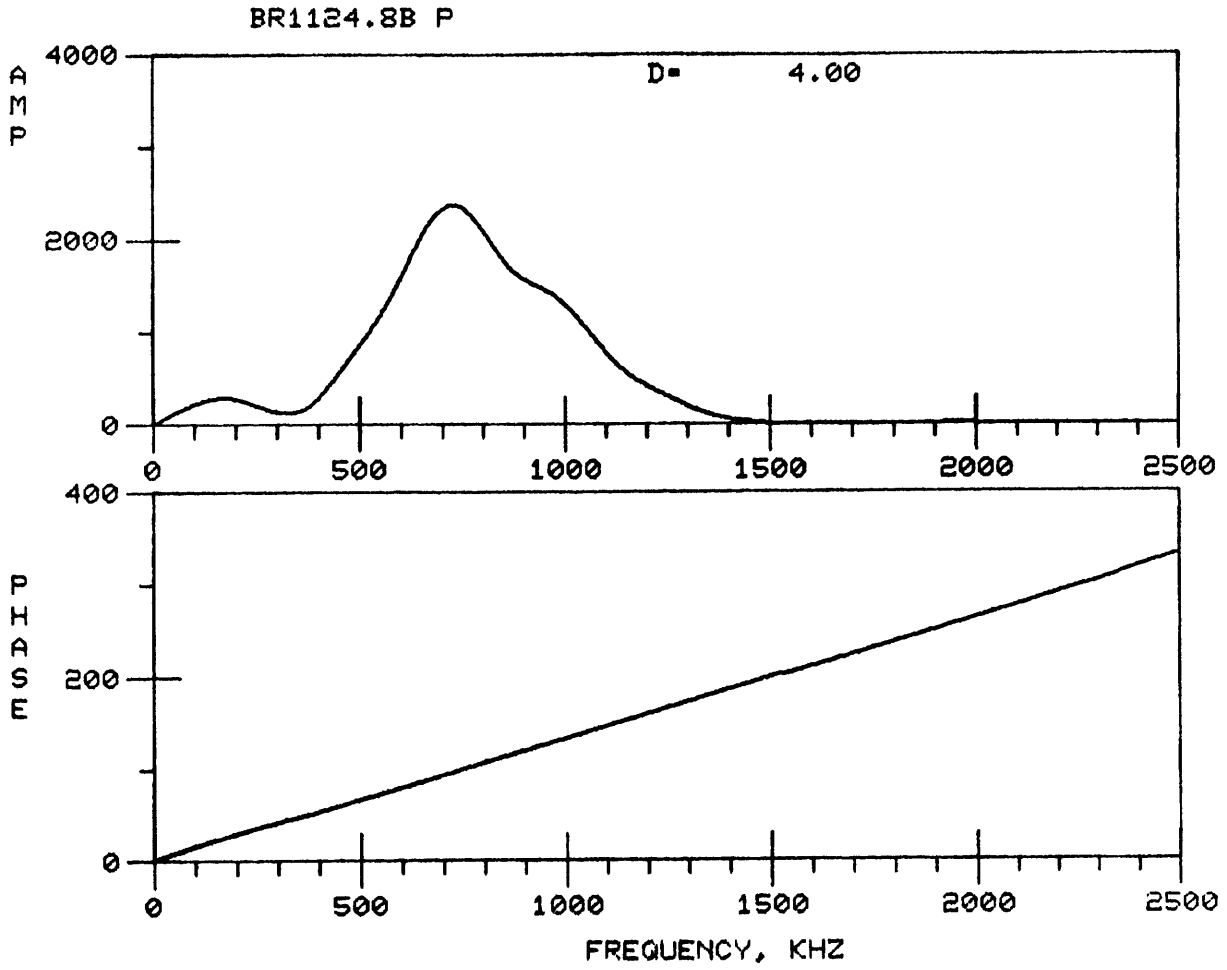
BR1124.8B P
D= 4.00
AMP
4000
2000
0
0
500
1000
1500
2000
2500
PHASE
400
200
0
0
500
1000
1500
2000
2500
FREQUENCY, KHZ

Figure 27

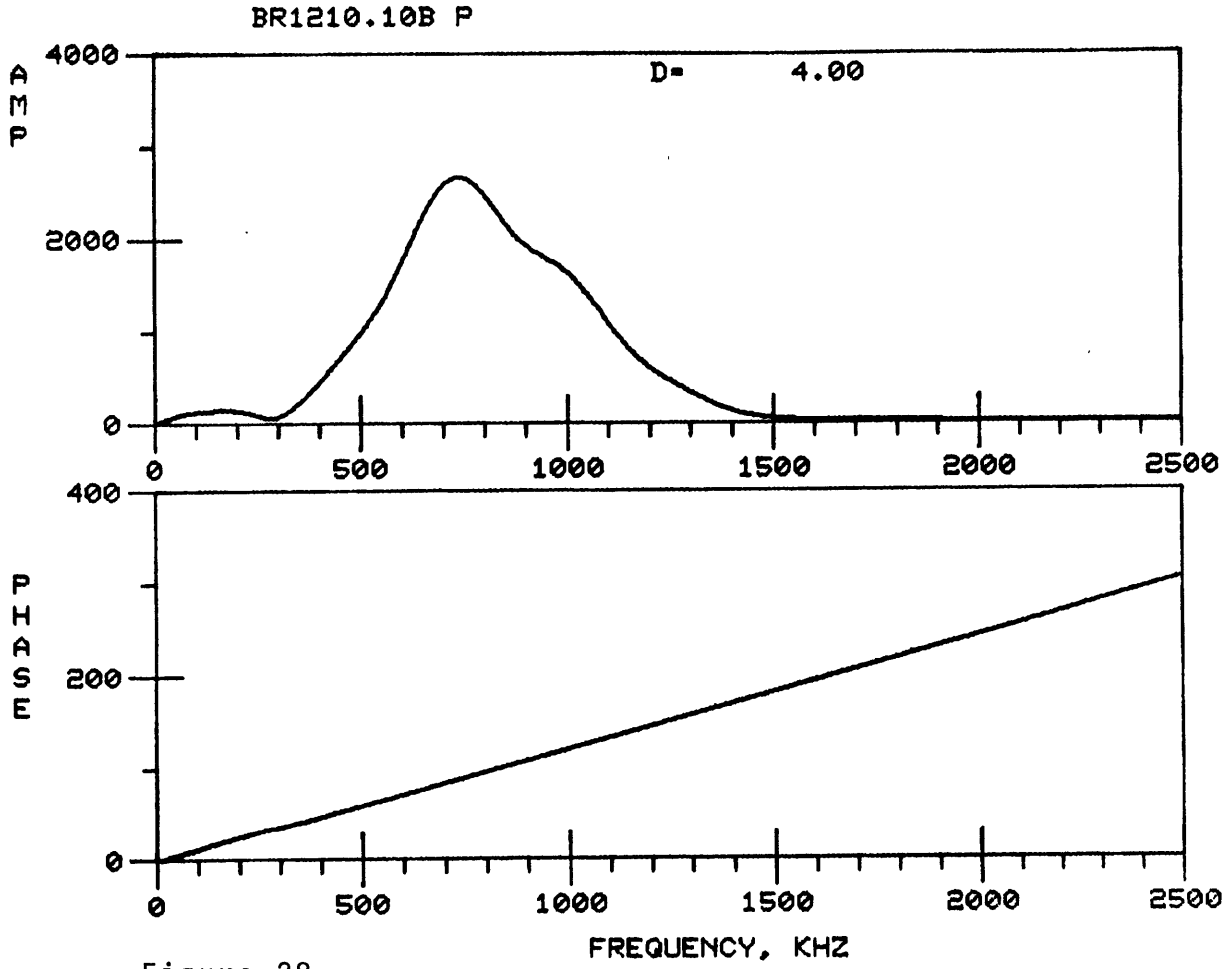
BR1210.10B P
D= 4.00
AMP
4000
2000
0
0
500
1000
1500
2000
2500
PHASE
400
200
0
0
500
1000
1500
2000
2500
FREQUENCY, KHZ

Figure 28

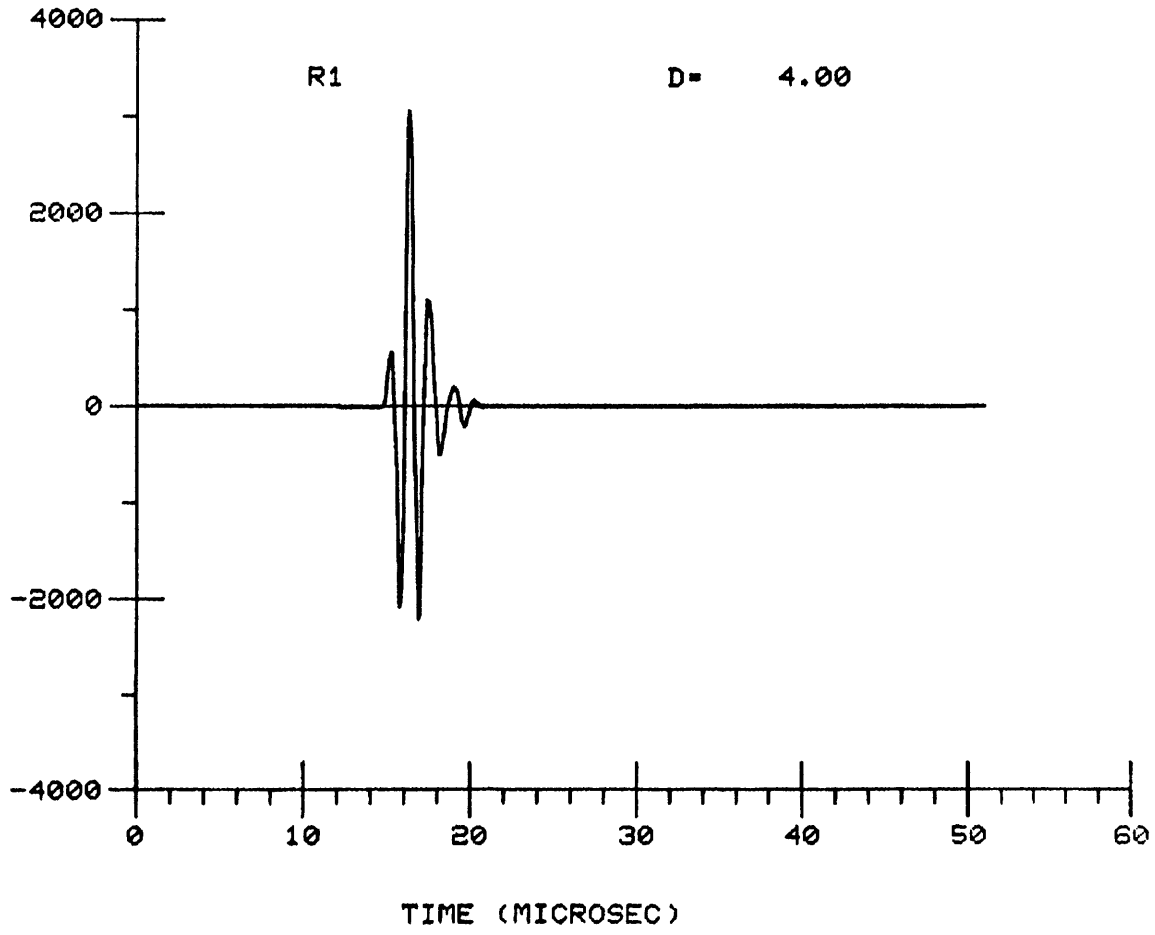

Figure 29

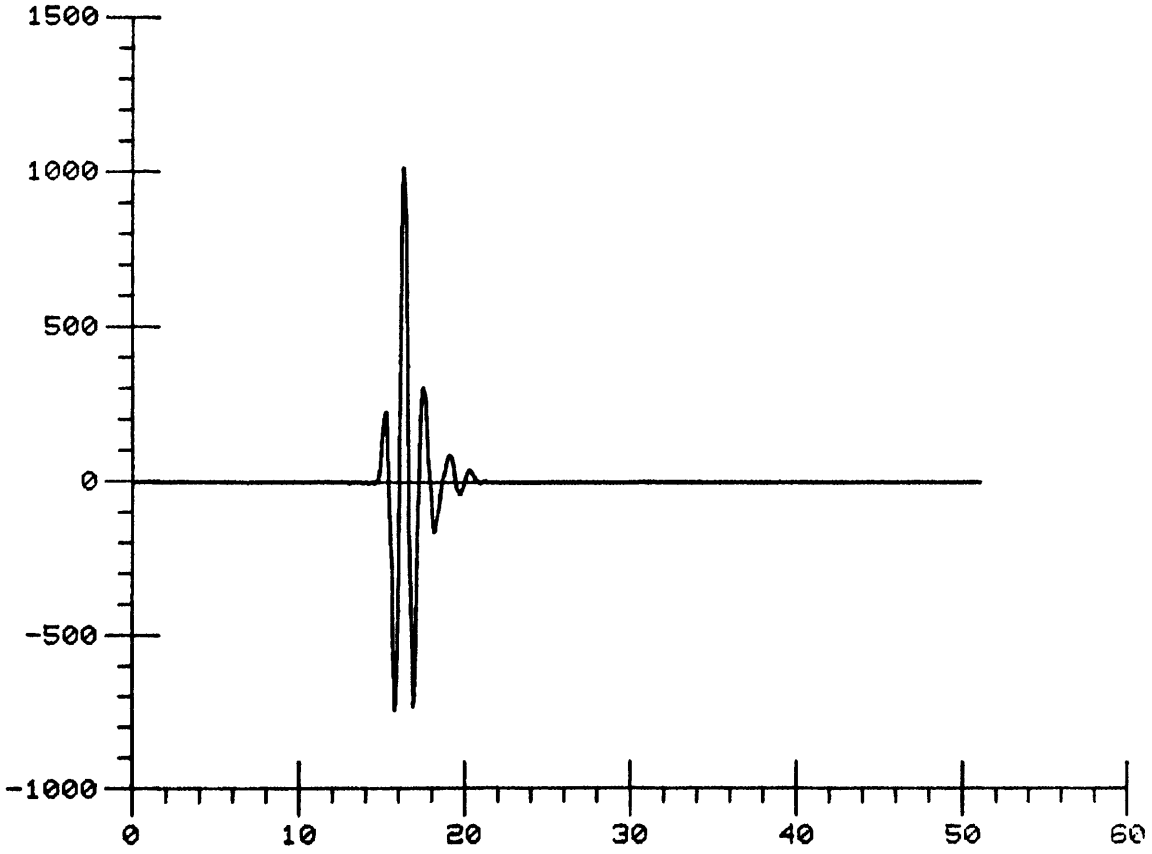

Figure 30

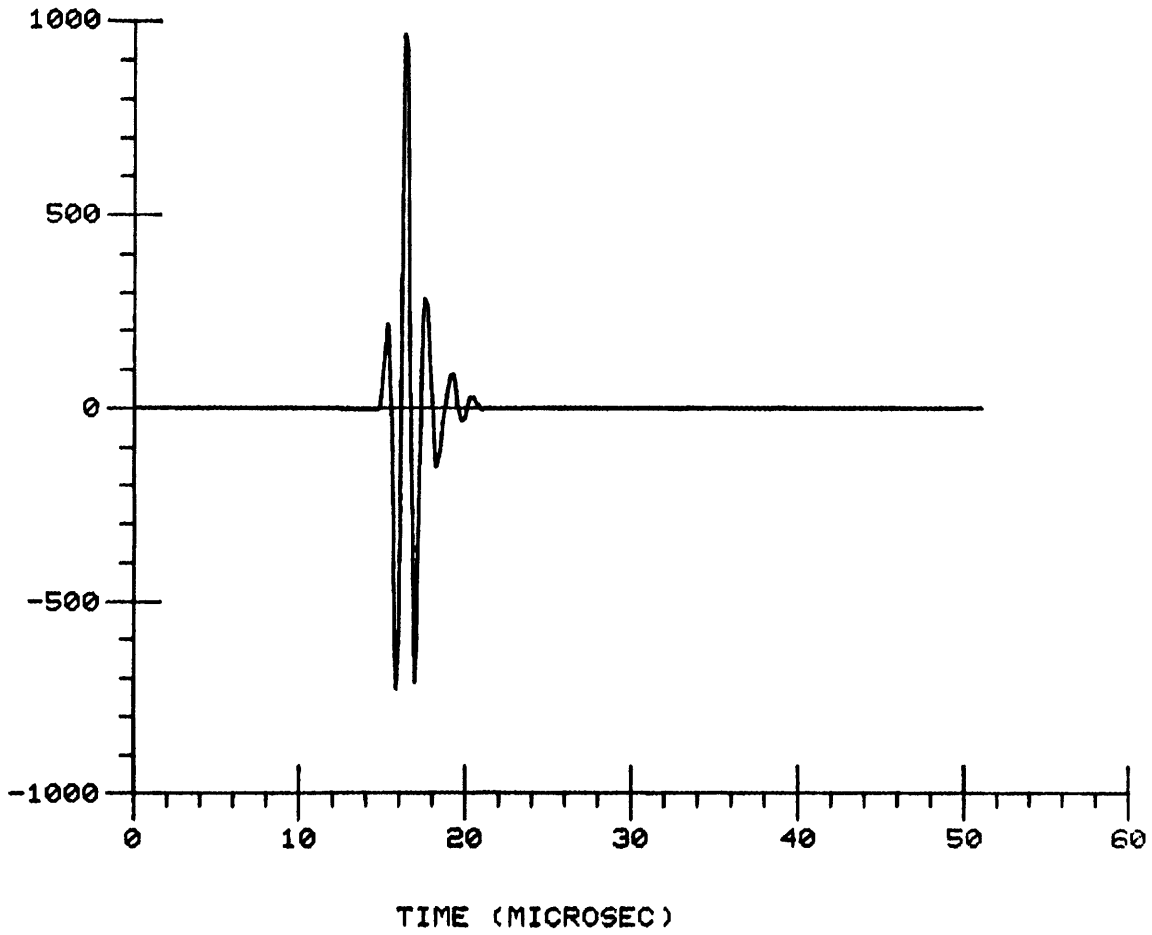

Figure 31

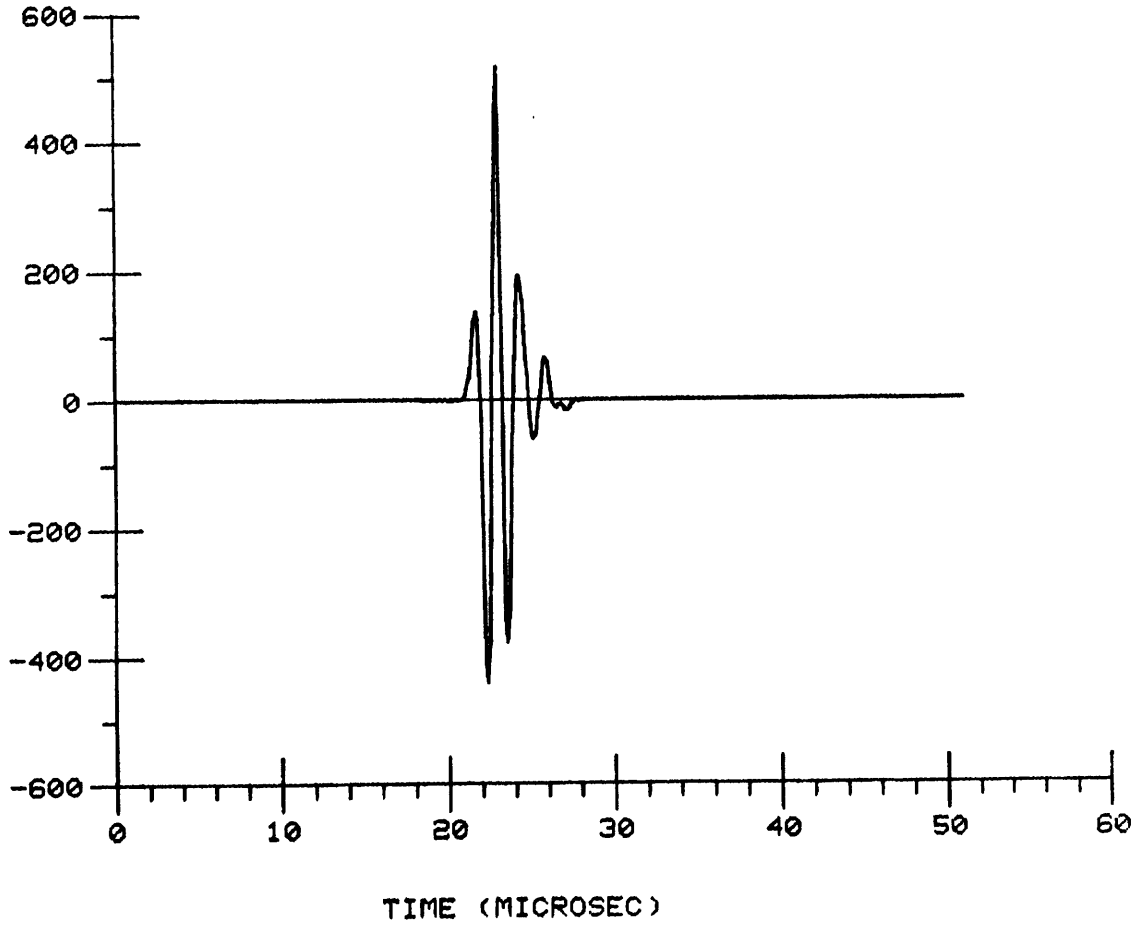

Figure 32

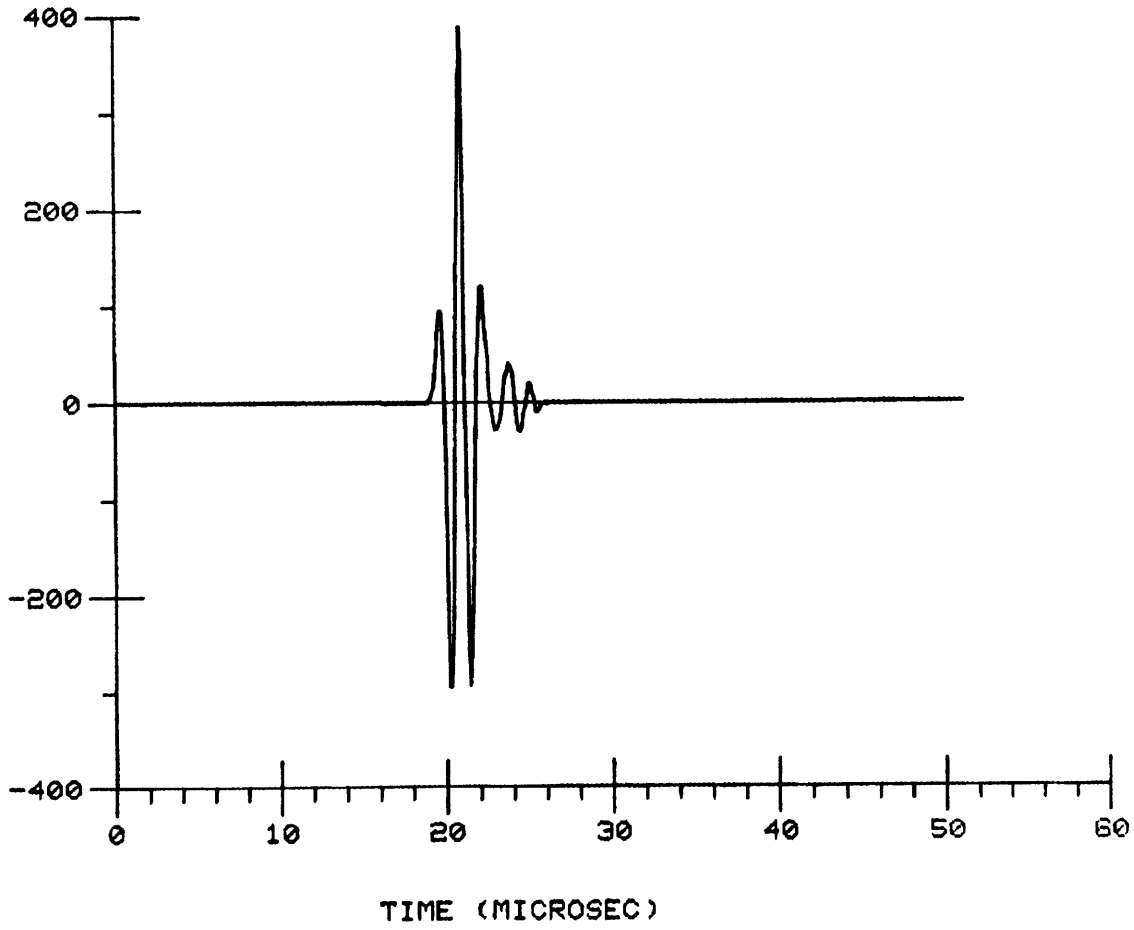

Figure 33

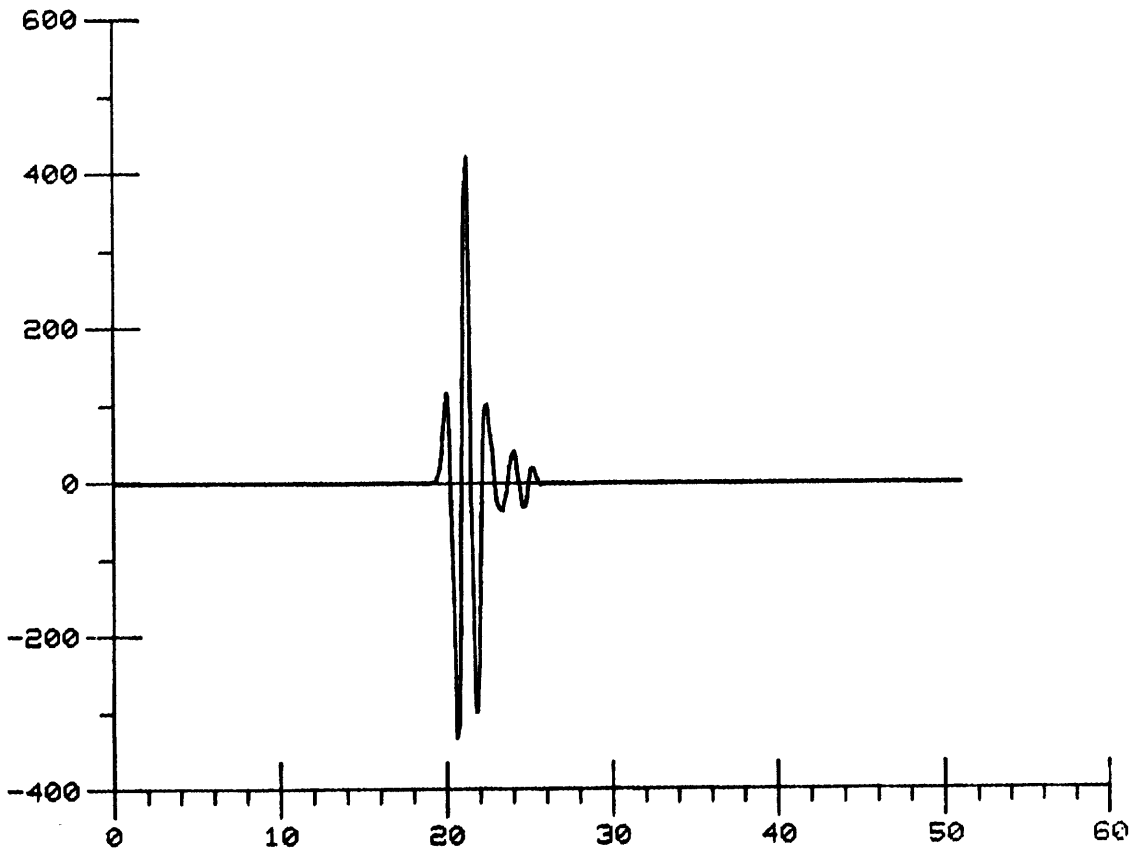

Figure 34

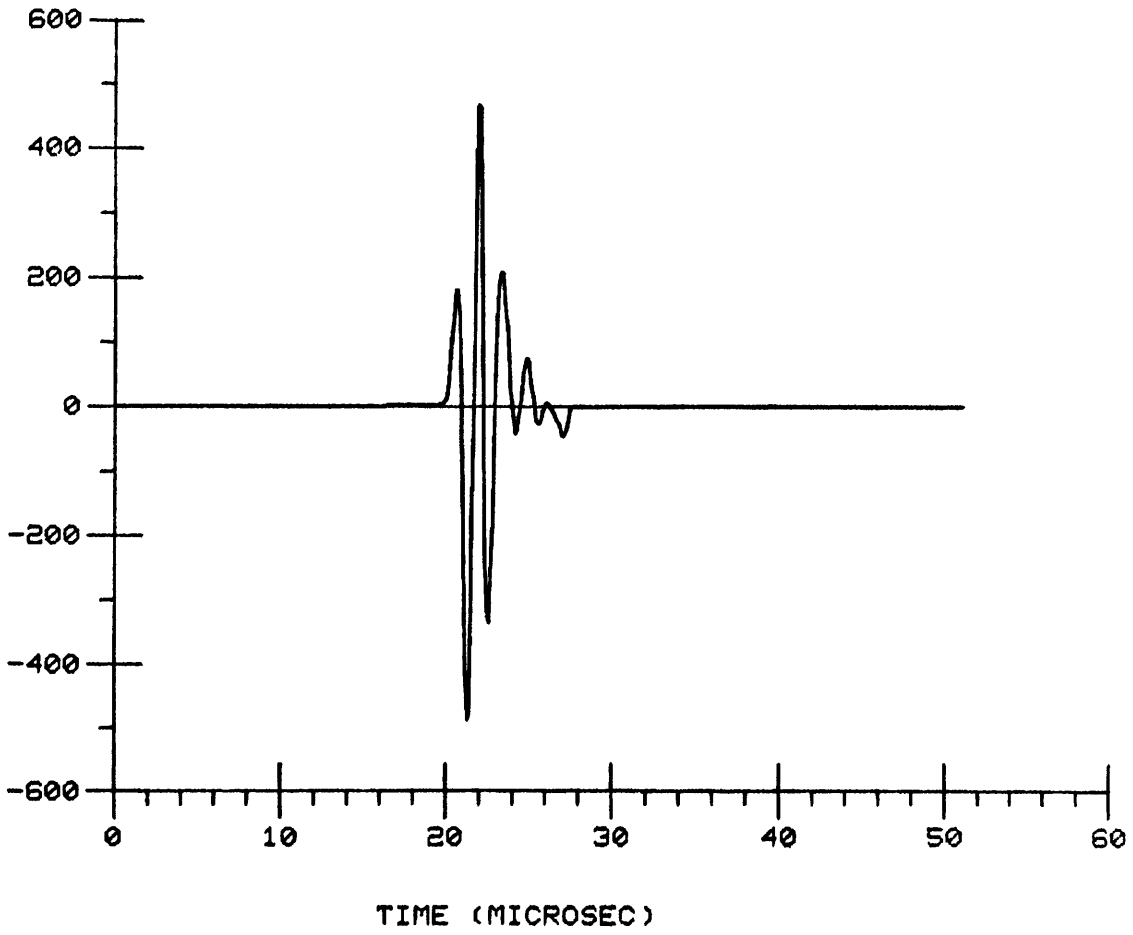

Figure 35

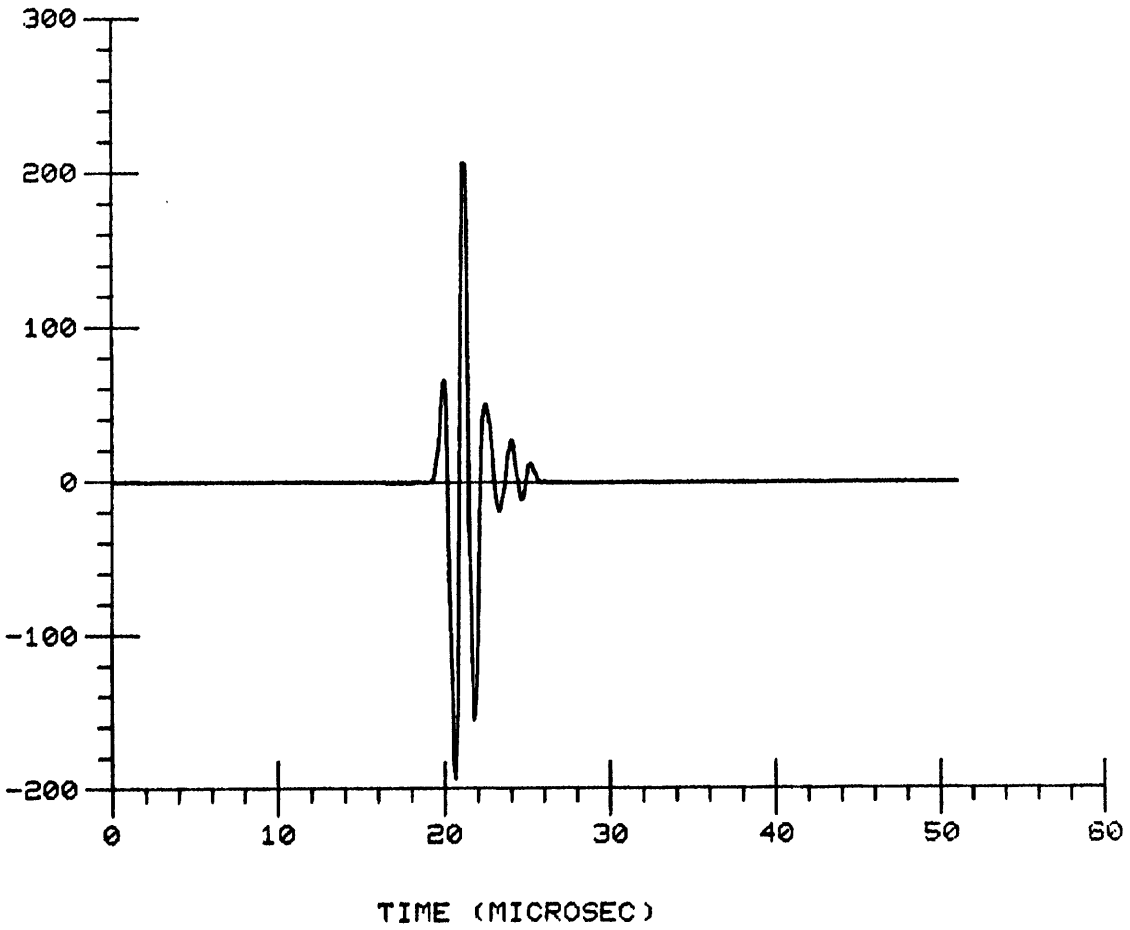

Figure 36

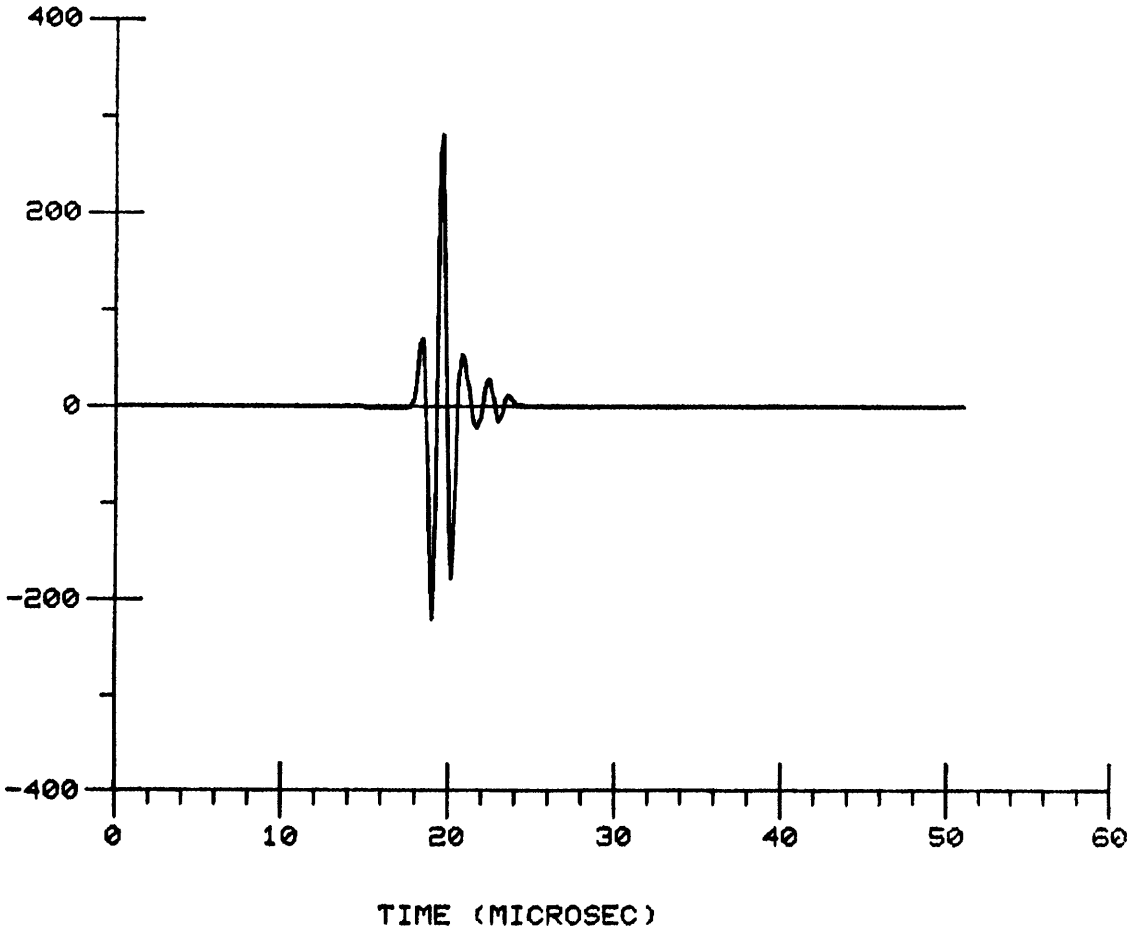

Figure 37